



UNIVERSITÀ
DI SIENA
1240

DIPARTIMENTO DI
**SCIENZE FISICHE, DELLA TERRA
E DELL'AMBIENTE**
— DSFTA

Ph. D. in Experimental Physics – XXXVII cycle

Optical Refrigeration: perspectives for the 2 micron region and new architectures for 1 micron applications

Supervisors: prof. Alberto Di Lieto
prof. Mauro Tonelli

Candidate: Francesco Caminati

Siena | 22/05/2025

List of contents

- Introduction
- Theoretical background
- Crystal Growth
- Optical Characterization
- Laser Sources
- Optical refrigeration experiments (LITMoS)
- Parallel configuration
- Cryostat for temperature-controlled LITMoS
- Conclusions

Optical Refrigeration Overview

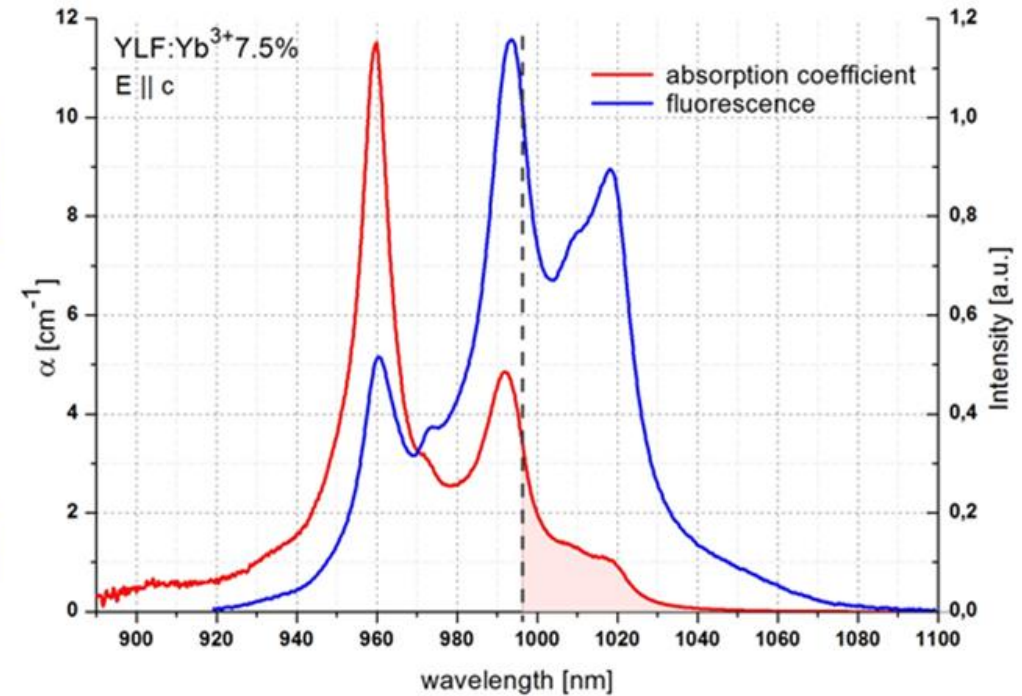
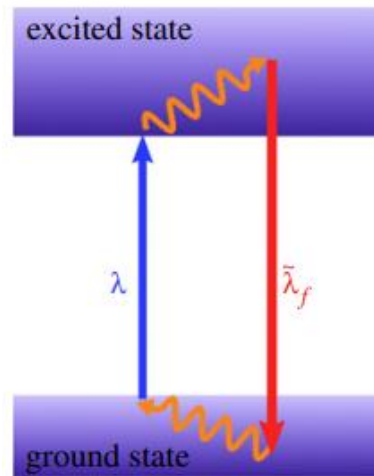
Anti-Stokes fluorescence:

$$\lambda > \lambda_f$$

Fluorescence emission subtracts energy from the system (phonon absorption).

Requirements:

- High host purity (fluoride crystals)
- Dopant with a high quantum efficiency transition and an overlap between absorption and fluorescence spectra at wavelengths longer than the mean fluorescence one (rare earth ions)



Left: sketch of the anti-Stokes refrigeration cycle (taken from [1]).

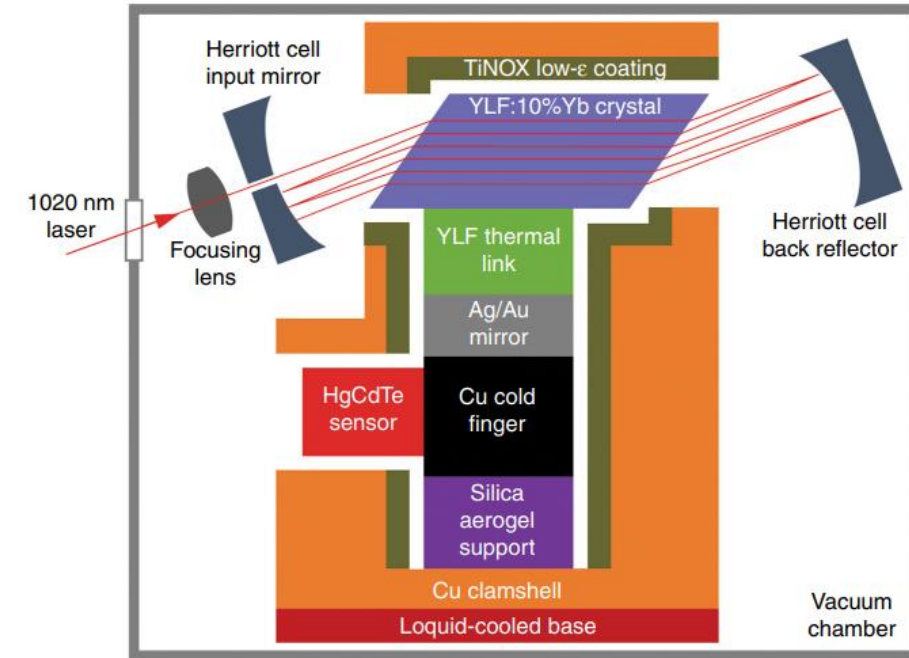
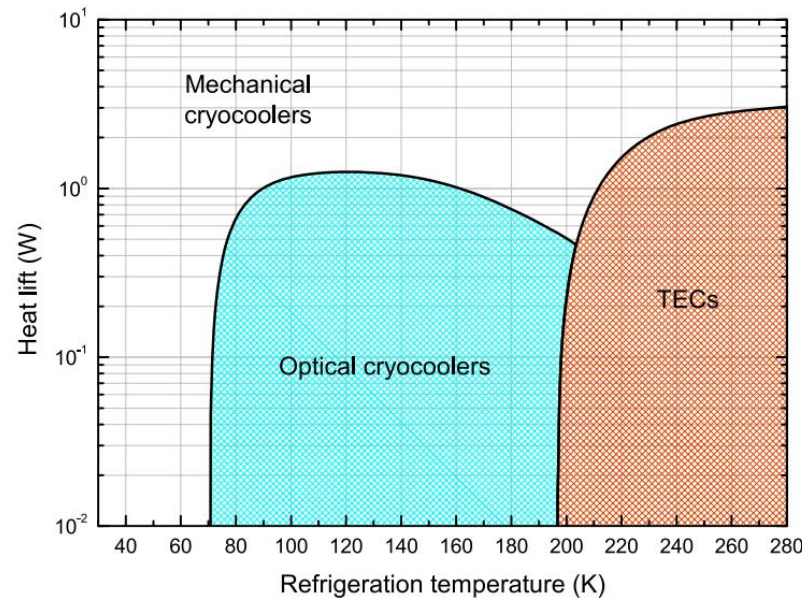
Right: absorption and emission spectra for Yb:YLF, with the overlap necessary for optical refrigeration.

All-solid-state cryocooler

Advantages:

- Compact design
- No moving parts → no vibrations
- long operational lifespan
- No magnetic interferences

Main application: cooling system for satellite components

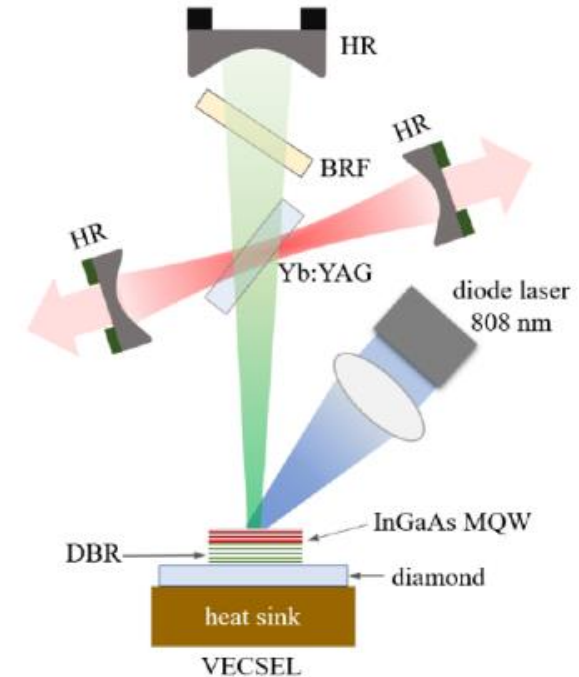


Left: Operational ranges and heat lift capacities of different types of coolers. Taken from B. C. Edwards, et al, "Development of the los alamos solid-state optical refrigerator". Review of scientific instruments, 69:2050-2055, 1998.

Right: First prototype of an all-solid state cryocooler. Taken from M. P. Hehlen, et al., "First demonstration of an all-solid-state optical cryocooler", Light: Science & Applications, 7, 2018.

Other applications

- **Radiation-balanced lasers:** intra-cavity cooling to reduce heating in operational laser sources by using a fraction of the laser power within the laser cavity;
- **Integrated coolers for data centers:** use solid state coolers in integrated circuits instead of air/water cooling systems to increase cooling efficiency of critical components (<https://mxllabs.com/maxwell-labs-announces-cooperative-research-development-agreement-with-sandia-labs-and-the-university-of-new-mexico-to-demonstrate-laser-cooling-for-high-density-processors/>).



Schematic of an intracavity-pumped radiation balanced disk laser setup (taken from Zhou Yang, et al., "Radiation-balanced Yb:YAG disk laser," Opt. Express 27, 1392-1400 (2019))

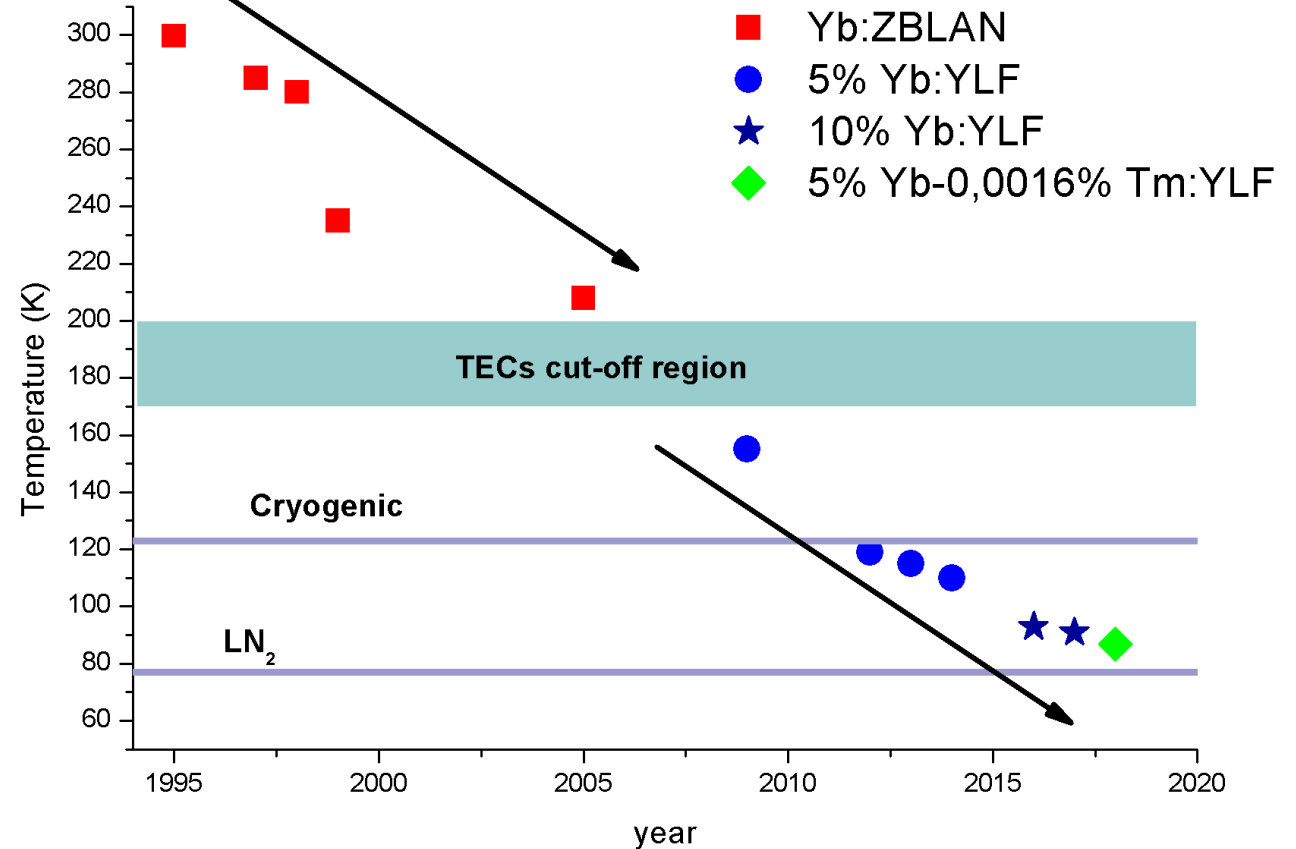
State of the art

Temperature record: 87 K for a LiYF_4 crystal sample doped with Ytterbium and Thulium, or **Yb,Tm:YLF** (A. Gragossian, et al., “Optical refrigeration inches toward liquid-nitrogen temperature“, SPIE newsroom, pages 2-4, 2017):

- Pump power: 50 W
- Multipass cavity: 30+ passages inside the sample
- $\Delta T = -193 \text{ K}$

Exploration of new materials:

- other fluoride crystal hosts (BaY_2F_8 , LiLuF_4 , KYF_4 , CaF_2 , SrF_2 , YAG.)
- other active ions (Tm, Ho, Cr)
- semiconductors



Fluoride crystals

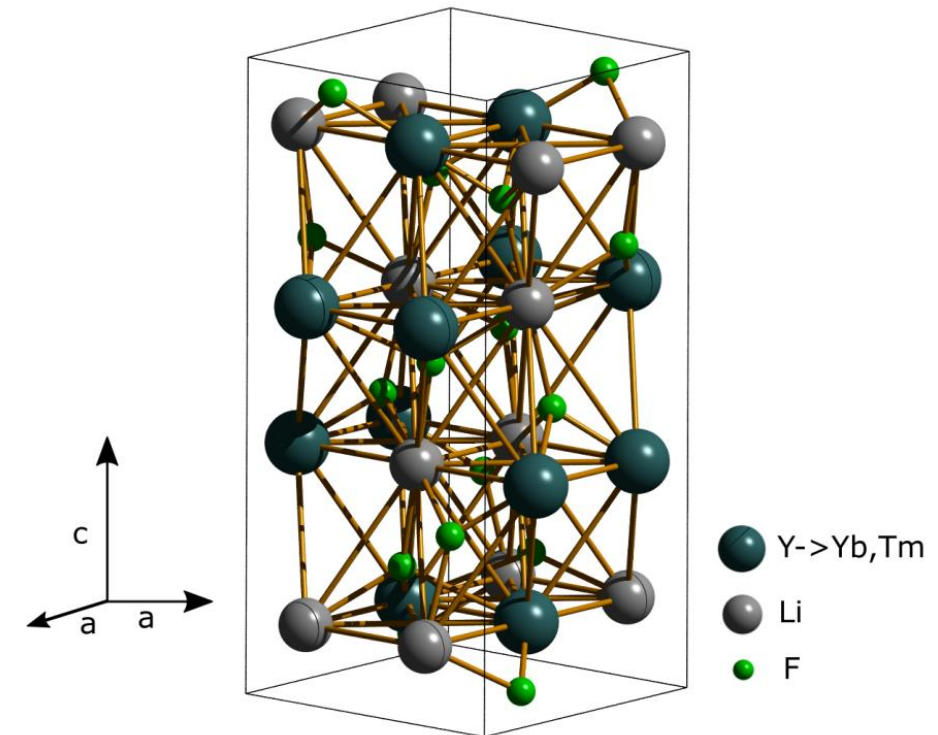
- Large energy gap (~ 11 eV)
- Low phonon energies ($350 - 500$ cm $^{-1}$)
- Large interstitial sites

LiYF₄ (YLF):

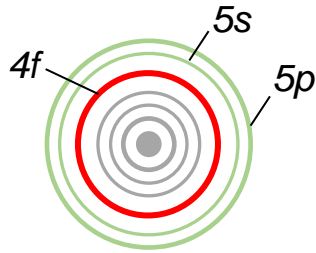
- Tetragonal lattice
- Uniaxal
- $Y^{3+} \rightarrow RE^{3+}$

Right: Yttrium Lithium Fluoride (YLiF₄, or YLF) unitary cell model.

Left: boules of fluoride monocrystals doped with rare earth elements (from www.megamaterials.it)



Rare earth elements

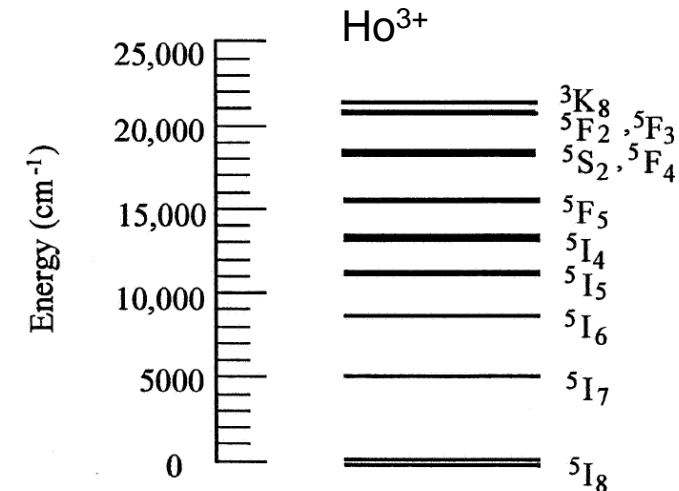
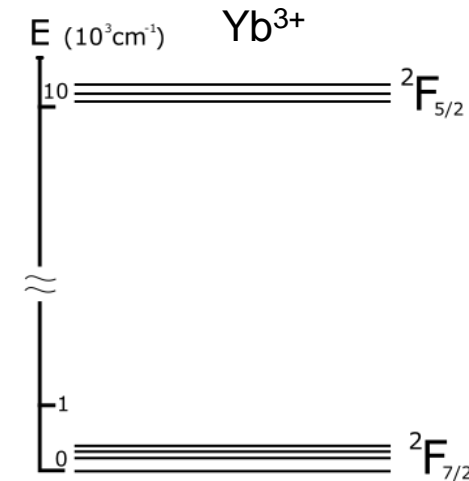


21 Sc
39 Y

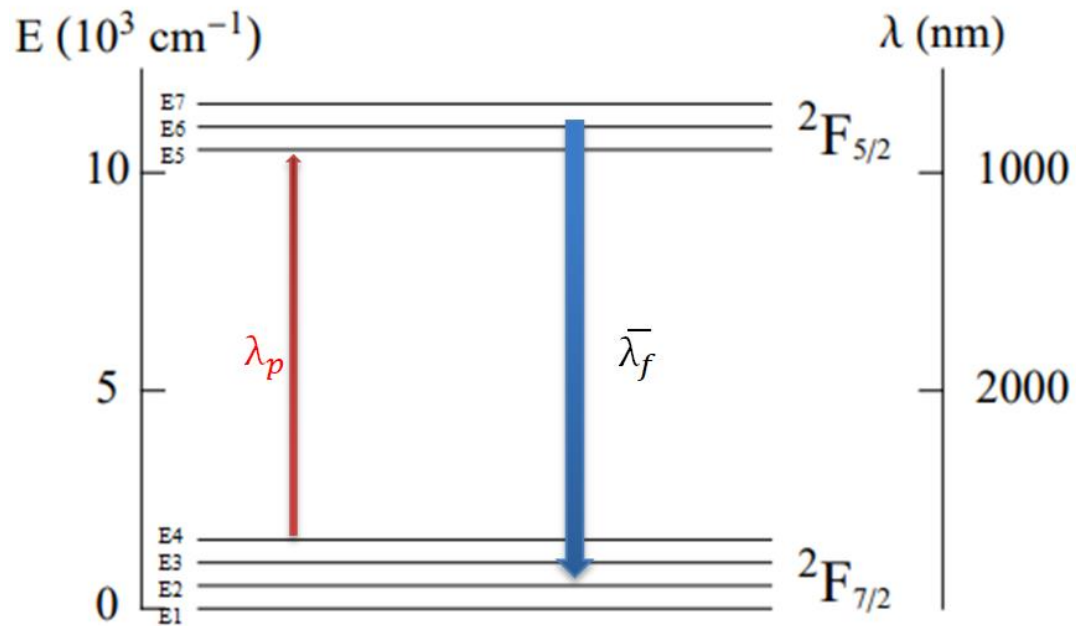
57 La Lanthanum 138.9055	58 Ce Cerium 140.115	59 Pr Praseodymium 140.90765	60 Nd Neodymium 144.24	61 Pm Promethium 144.9127	62 Sm Samarium 150.36	63 Eu Europium 151.9655	64 Gd Gadolinium 157.25	65 Tb Terbium 158.92534	66 Dy Dysprosium 162.50	67 Ho Holmium 164.93032	68 Er Erbium 167.26	69 Tm Thulium 168.93421	70 Yb Ytterbium 173.04	71 Lu Lutetium 174.967
-----------------------------------	-------------------------------	---------------------------------------	---------------------------------	------------------------------------	--------------------------------	----------------------------------	----------------------------------	----------------------------------	----------------------------------	----------------------------------	------------------------------	----------------------------------	---------------------------------	---------------------------------

Rare Earth trivalent ion: $[Xe]4f^n$ with $n = 1-14$

- Valence electrons are screened by outer shells
- Weak ion interaction with the surrounding host
- Very narrow emission and absorption spectral lines



Optical refrigeration cycle



Example of the optical refrigeration cycle in Yb:YLF

$$\bar{\lambda}_f = \frac{\int \lambda I(\lambda) d\lambda}{\int I(\lambda) d\lambda}$$

$\lambda_p > \bar{\lambda}_f \rightarrow$ Emitted photons will extract energy from the system

Ideal refrigeration efficiency:

$$\eta_c = \frac{h\nu_f - h\nu}{h\nu} = \frac{\lambda}{\bar{\lambda}_f} - 1$$

Optical refrigeration efficiency

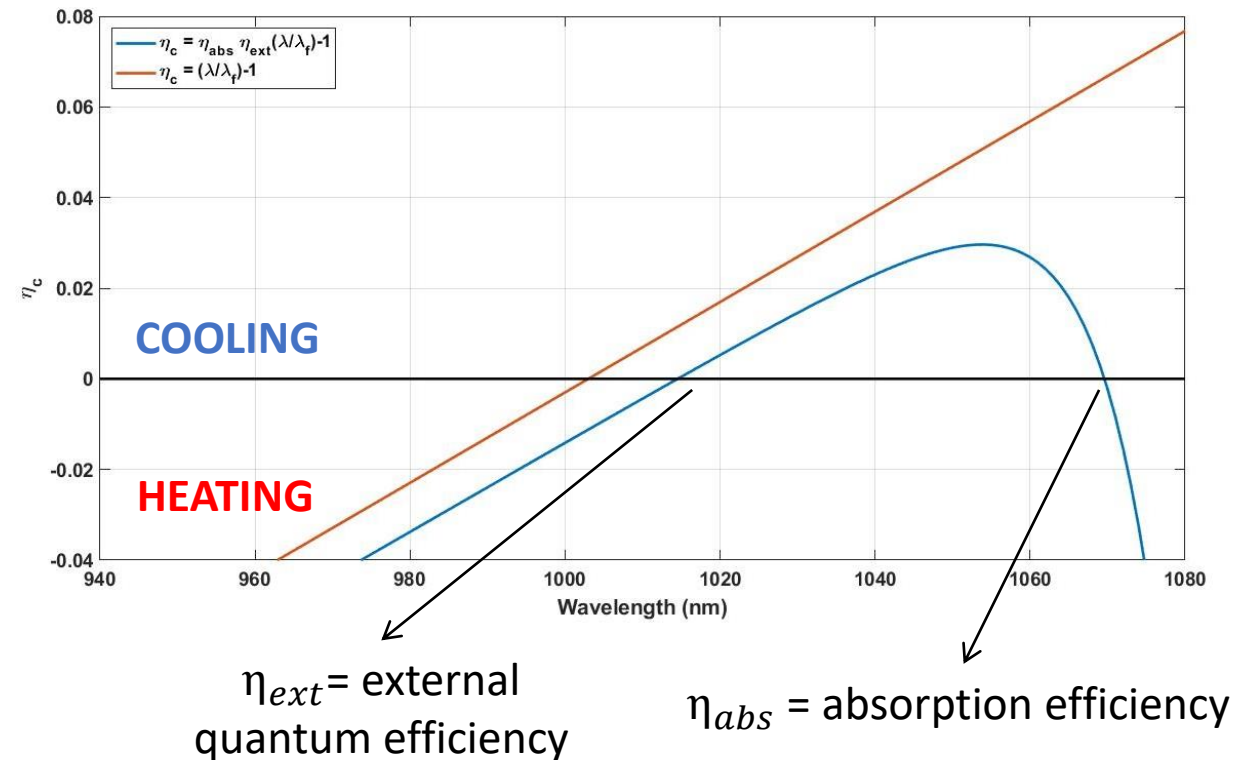
$$\cancel{\eta_c = \frac{\lambda}{\lambda_f} - 1} \rightarrow \eta_c = p(\lambda) \frac{\lambda}{\lambda_f} - 1 = \eta_{ext} \eta_{abs} \frac{\lambda}{\lambda_f} - 1$$

with

$$\eta_{abs} = \frac{\alpha_r(\lambda)}{\alpha_r(\lambda) + \alpha_b} \quad \eta_{ext} = \frac{\eta_e W_r}{\eta_e W_r + W_{nr}}$$

Phenomena that can reduce **the cooling efficiency**:

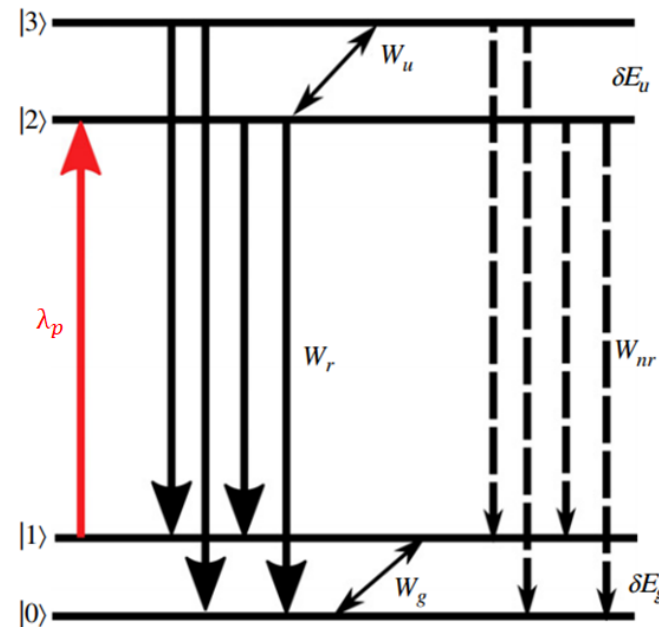
- Absorption from impurities (α_b)
- Non-radiative decays (W_{nr})
- Photon reabsorption (η_e)
- Radiation trapping, TIR (η_e)



Four level model

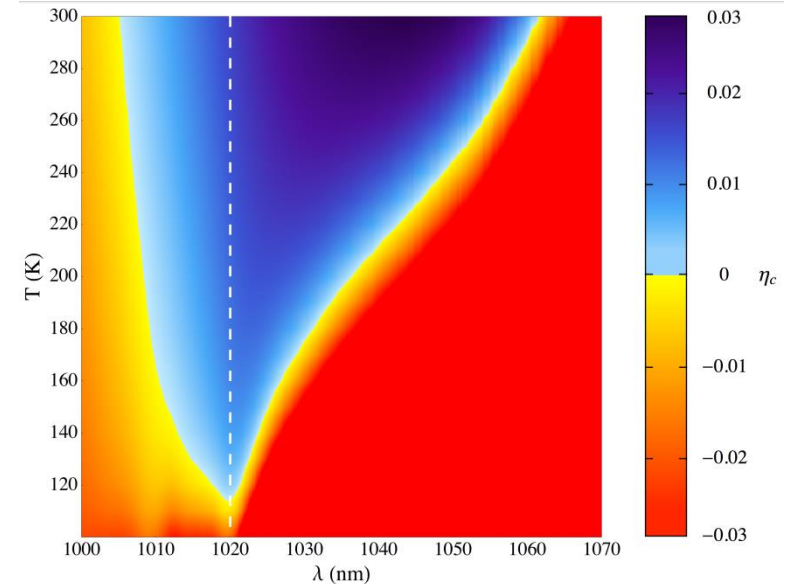
Four-level model: rate-equation-based model built on only five experimentally accessible macroscopic quantities:

- $\alpha_0(\lambda, T)$, the unsaturated resonant absorption
- $\bar{\lambda}_f(T)$, the mean fluorescence wavelength
- η_{ext} , the external quantum efficiency
- α_b , the parasitic background absorption
- I_s , the saturation intensity of a homogeneously broadened transition



Left: the scheme of the four level optical refrigeration model composed by a ground ($|0\rangle$, $|1\rangle$) and excited ($|2\rangle$, $|3\rangle$) state multiplets. Inter-multiplet recombination occurs via radiative (W_r , full arrows) or nonradiative (W_{nr} , dashed arrows) decay channels, after the excitation of the lowest-energy transition ($|1\rangle - |2\rangle$, red arrow). Adapted from [1]

Right: the Minimum Achievable Temperature (MAT) plot (white line) on a cooling efficiency estimation colormap for 5% Yb:YLF (taken from [2]).



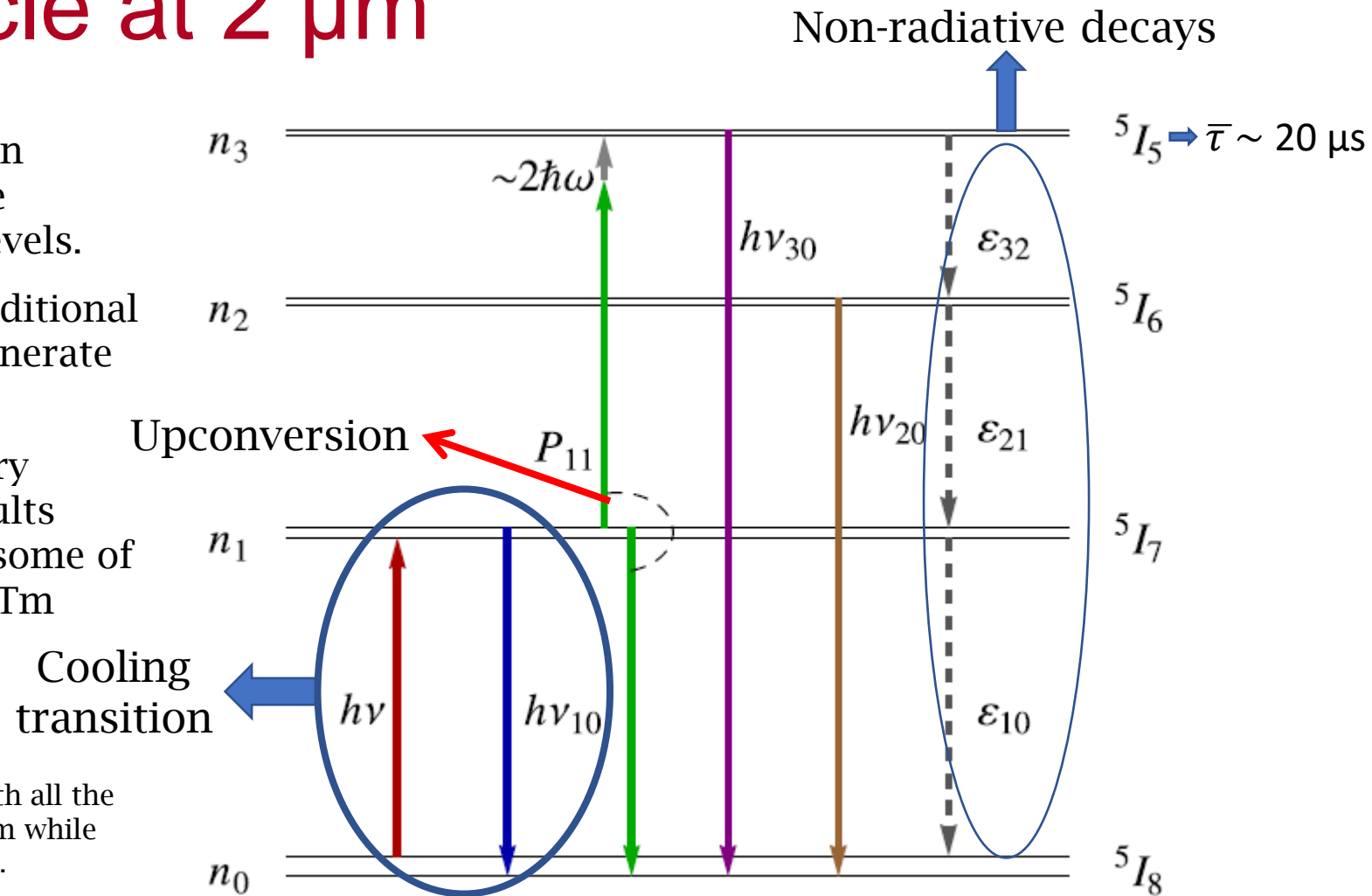
Refrigeration cycle at 2 μm

To represent the refrigeration cycle in Ho:YLF, the four level model must be expanded to involve higher energy levels.

These higher levels will introduce additional transitions, which will most likely generate additional heating of the system.

Simulations on such a system are very complex. Dong et al [3] obtained results which appear to be in contrast with some of the experimental results for Ho and Tm ions.

Scheme of the first four manifolds of Ho:YLF, with all the possible transitions that may occur between them while pumping with a laser (red arrow). Taken from [3].



Why shift to 2 μm ?

Low temperature record: 87 K for Yb,Tm:YLF

Problem of Yb:YLF

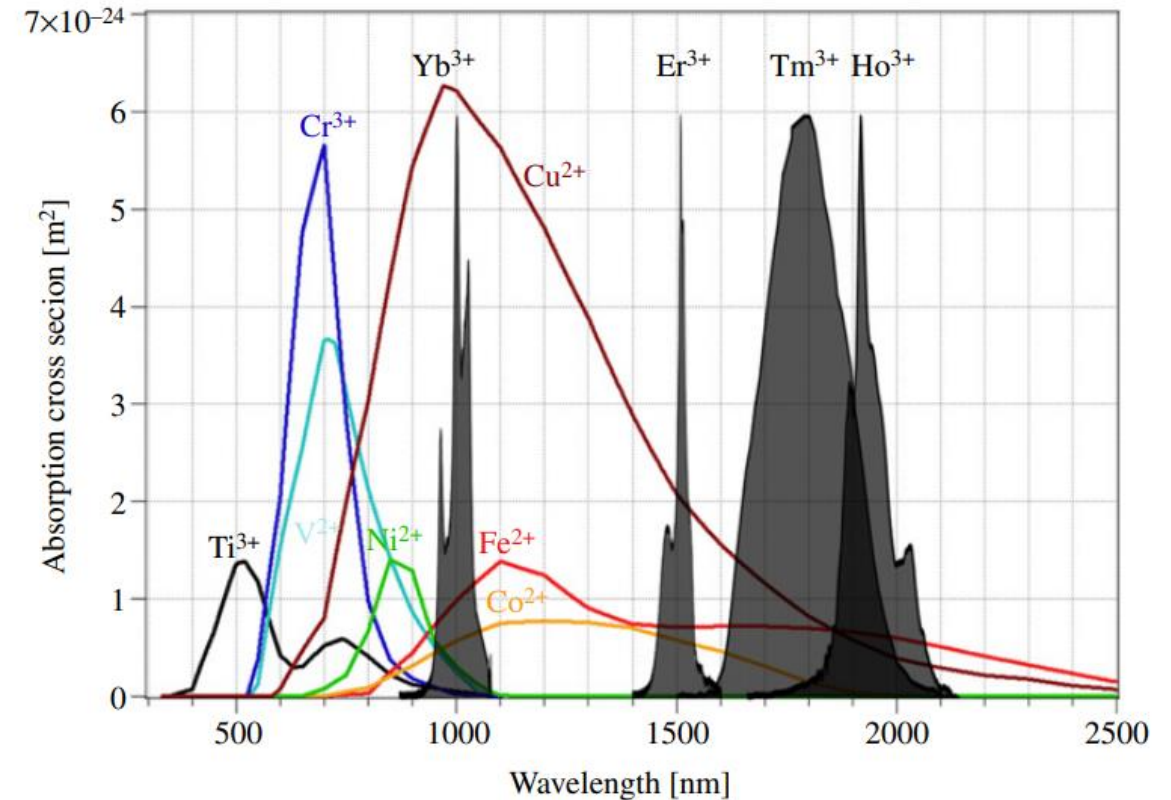
Results are not easily reproducible: individual samples with similar characteristics might cool down or not.

Cause

Small amounts of unwanted and uncontrollable impurities lower the cooling efficiency (transition metals).

Shift to 2 μm :

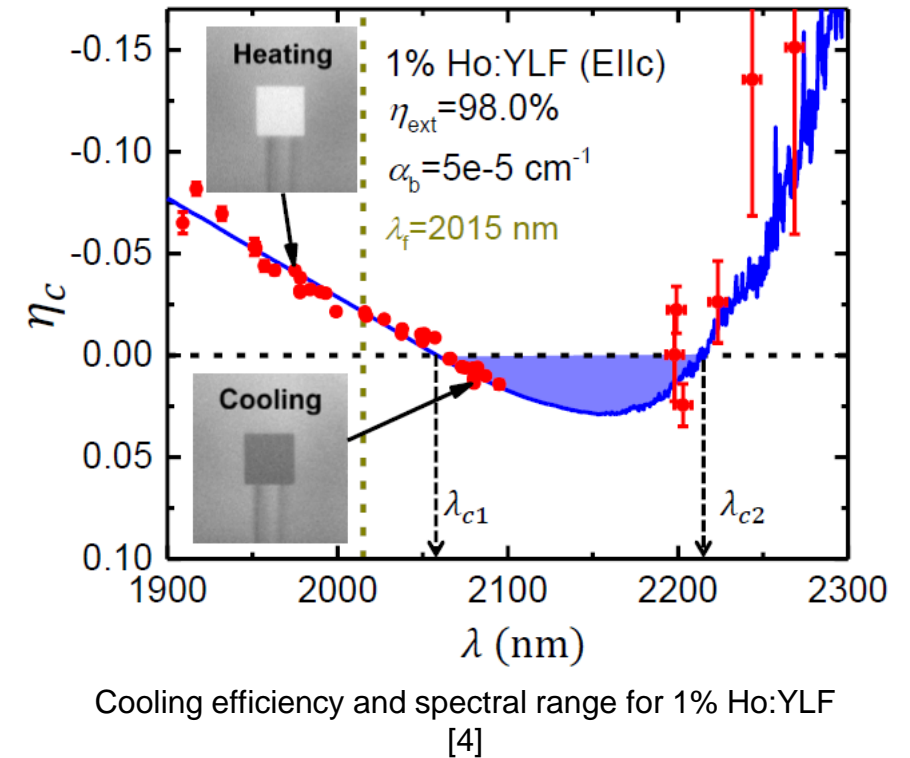
- Longer wavelengths = higher efficiency;
- No transition metal absorption.



Comparison of the absorption cross-section of various transition metals in fluoride glasses, compared to the cross-section of certain rare earth elements (taken from [1]).

Objectives

- Grow Ho:YLF crystal boules with different doping levels (0,8% and 1%);
- Characterize the optical properties of the samples (absorption, fluorescence, mean lifetimes);
- Build a 2 μm tunable laser source ($P_{\text{out}} \approx 0,5 \text{ W}$ at $\lambda = 2050 - 2100 \text{ nm}$);
- Test the optical refrigeration performances of Ho:YLF samples around 2070-2100 nm;
- Explore new designs (the parallel configuration);
- Design of a cryostat for temperature-controlled LITMoS experiments (at Institut Néel, CNRS, Grenoble, France);



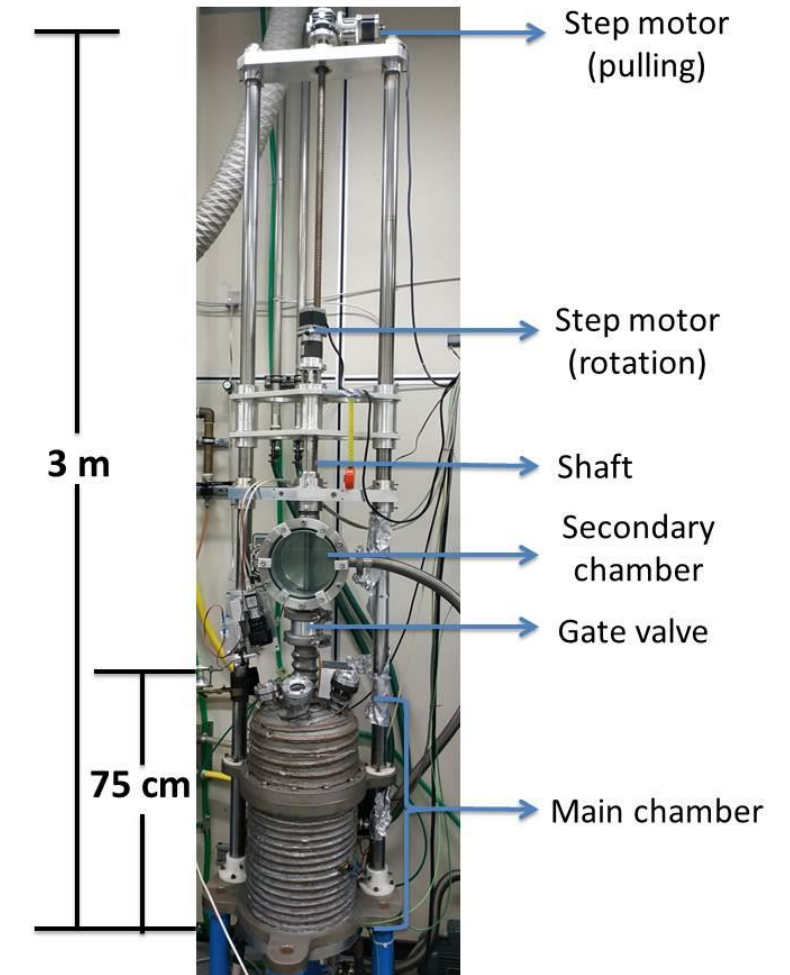
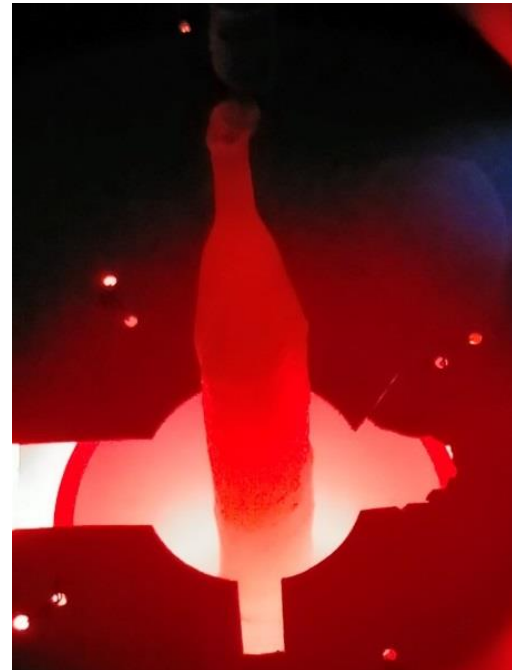
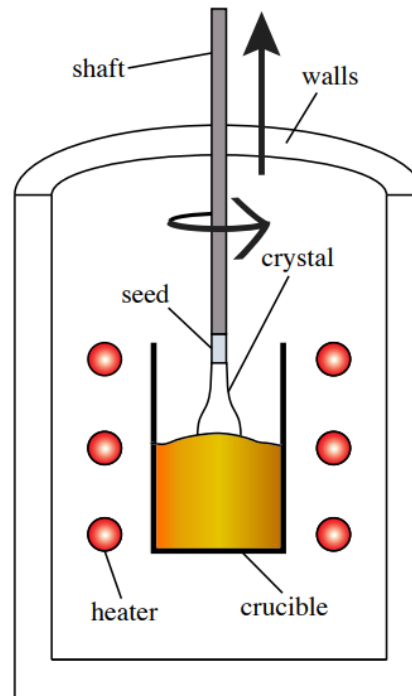
Growth of Ho:YLF monocrystals

- The Czochralski technique
- Growth procedure
- Preparation of the crystal samples

Crystal growth

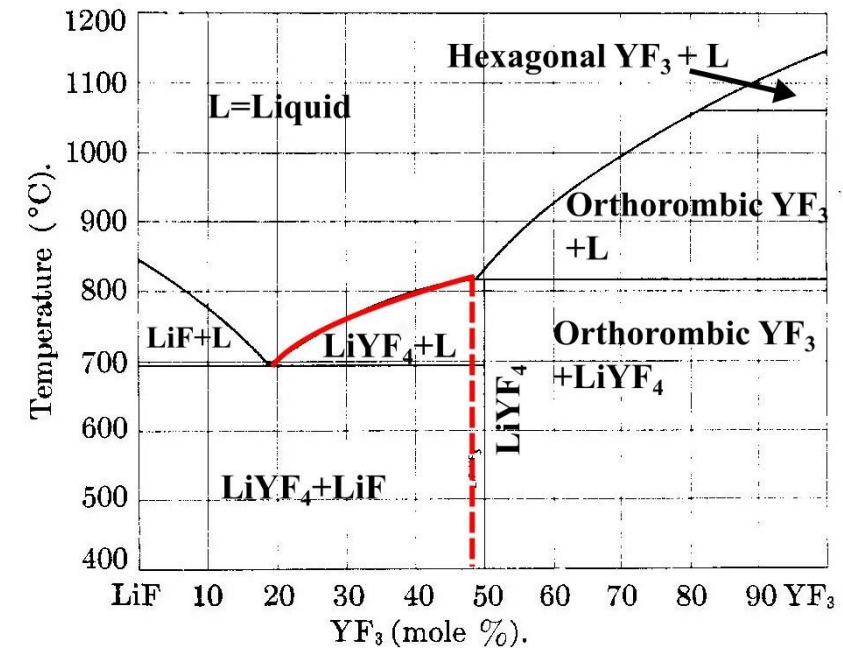
All the crystal samples used in this project were obtained from crystal boules grown in the University of Pisa laboratories using the Czochralski technique.

Left: scheme of a Czochralski furnace;
Center: a Ho:YLF boule growing inside the furnace;
Right: one of the University of Pisa furnaces, with its main components.



Growth procedure

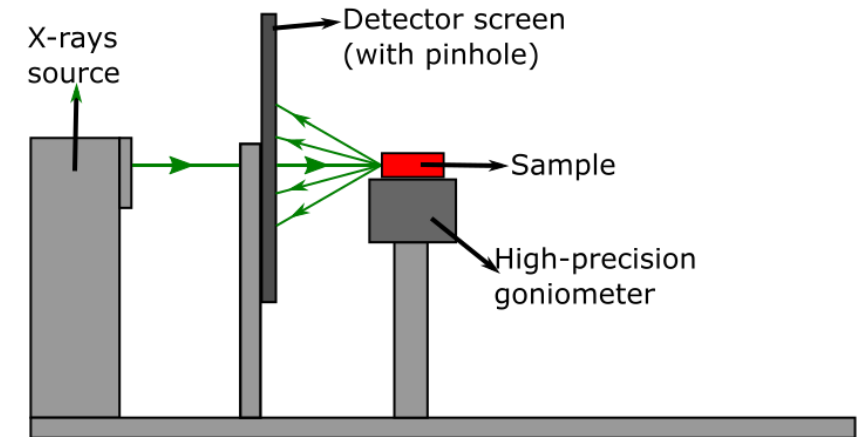
- «Baking» of the furnace
- Weighting of the components (5N powders)
- Creation of a vacuum
- Addition of 5N inert gases (and some CF_4 for Yb)
- Melting of the powders
- Cleaning the melt
- Contacting with the seed
- Pulling and rotation
- Extraction of the boule



Phase diagram for YLF

Sample preparation

- Boule orientation (polarizers + Laue scattering analysis)
- Preliminary cut
- Check for impurities with a laser and a microscope
- Final sample cut
- Optical-grade polishing



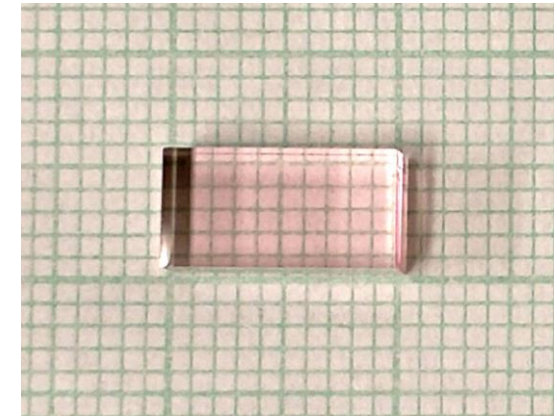
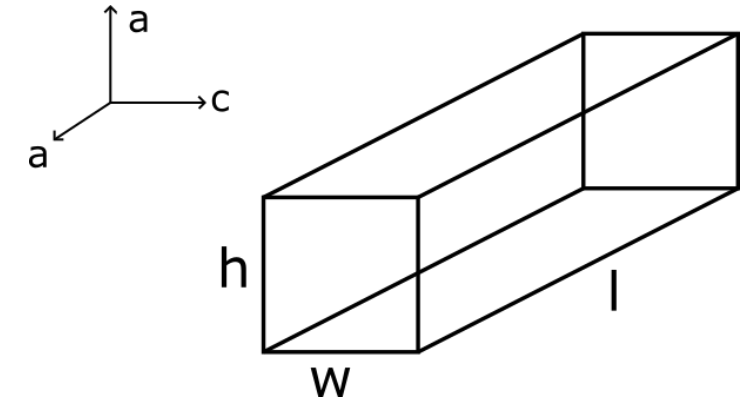
Top: scheme of the X-ray machine for Laue scattering analysis;

Bottom: The last 1% Ho:YLF boule that was grown during this project (boule #3).



Ho:YLF boules and samples

Material	Boule	Sample	Size
0,8% Ho:YLF	Boule 1	Sample 1	5,9 (c) x 6,4 (a) x 8,9 (a) mm ³
		Sample 2	5,9 (c) x 5,3 (a) x 5,5 (a) mm ³
		Sample 3	5,1 (c) x 4,8 (a) x 4,8 (a) mm ³
1% Ho:YLF	Boule 2	Sample 4	5,0 (c) x 5,0 (a) x 9,8 (a) mm ³
		Sample 5	5,1 (c) x 5,1 (a) x 8,0 (a) mm ³
	Boule 3	Sample 6	5,0 (c) x 5,0 (a) x 11,2 (a) mm ³
		Sample 7	5,0 (c) x 5,0 (a) x 5,0 (a) mm ³



Top: table with all the Ho:YLF samples that were fabricated and tested;

Top right: scheme of the shape of a crystal sample;

Bottom right: picture of sample #4.

Optical characterization of Ho:YLF

- Absorption measurements
- Low temperature absorption measurements
- Fluorescence reabsorption measurements
- Low temperature fluorescence measurements
- Mean lifetime measurements

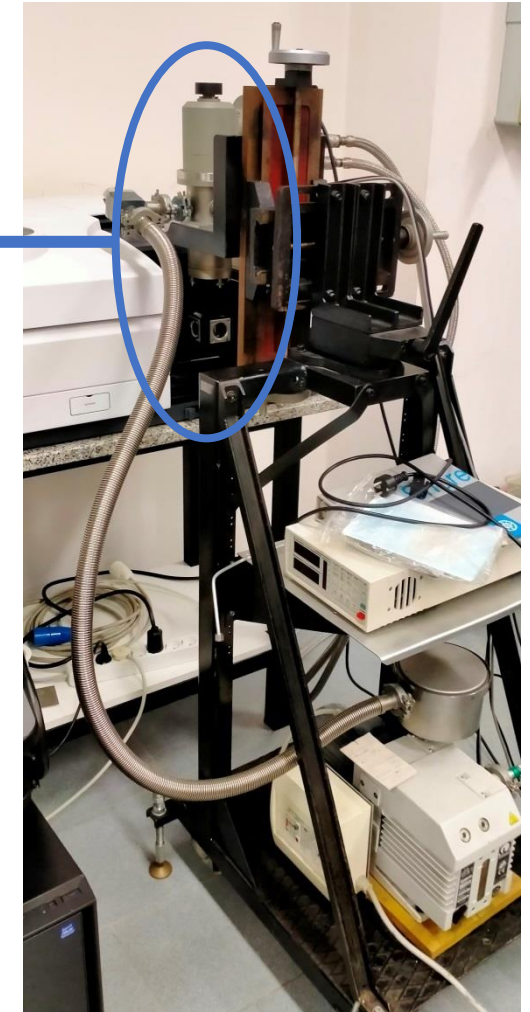
Absorption setup

Absorption measurements instrument:

- Cary 5000 UV/Vis/NIR spectrometer

For low temperatures, we added:

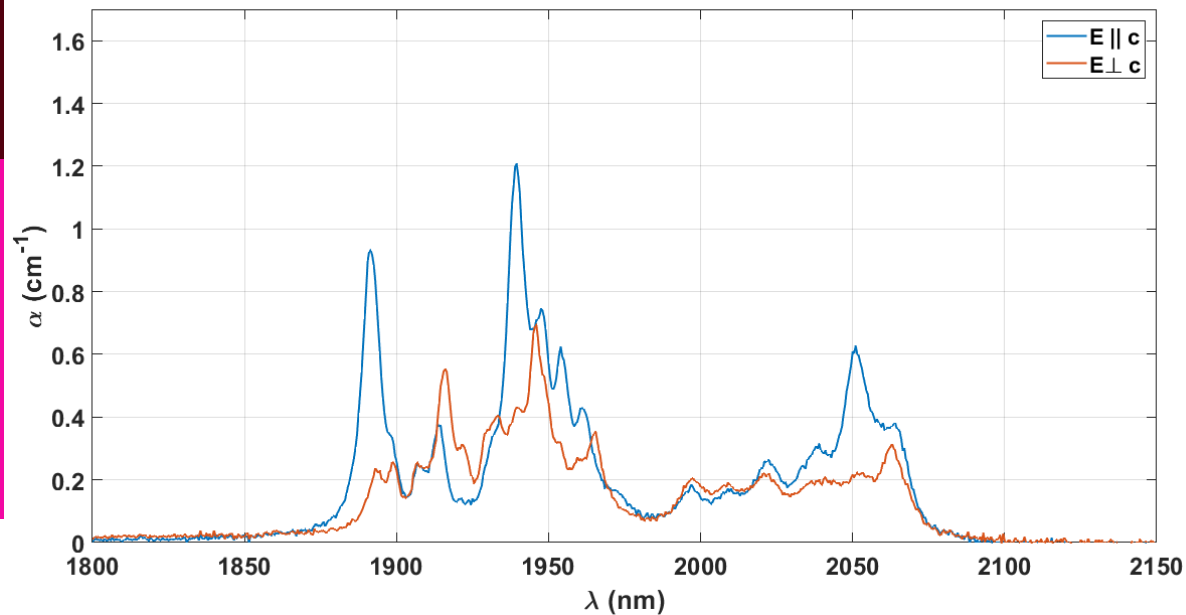
- Cryostat (with He compressor)
- Rotative pump
- Temperature controller
- Copper sample holder with $d=3$ mm pinhole



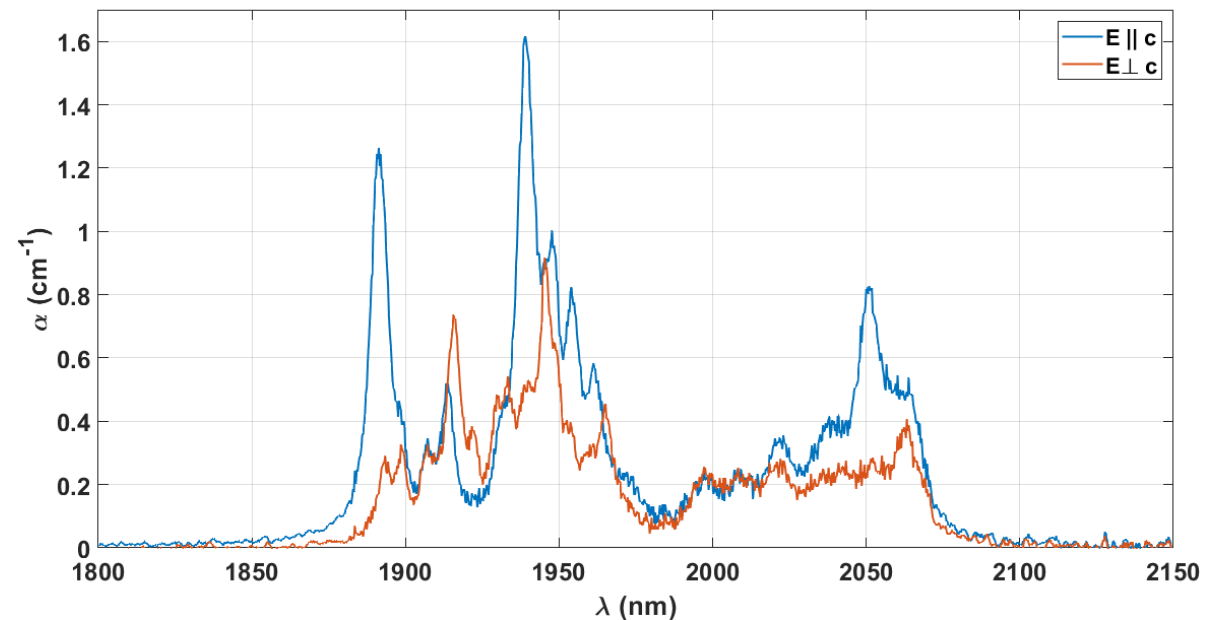
Left: Low-temperature absorption setup. On the background, there is the Cary 5000 spectrometer, into which we inserted cryostat connected to a vacuum pump, and a temperature controller;
Top: Detail of the cryostat itself.

Ho:YLF absorption results

- 0.8% Ho:YLF sample;
- Range: 1800 - 2150 nm;
- Step: 0,5 nm;
- Integration time: 2 s;



- 1% Ho:YLF sample;
- Range: 1800 - 2150 nm;
- Step: 0,3 nm;
- Integration time: 3 s;

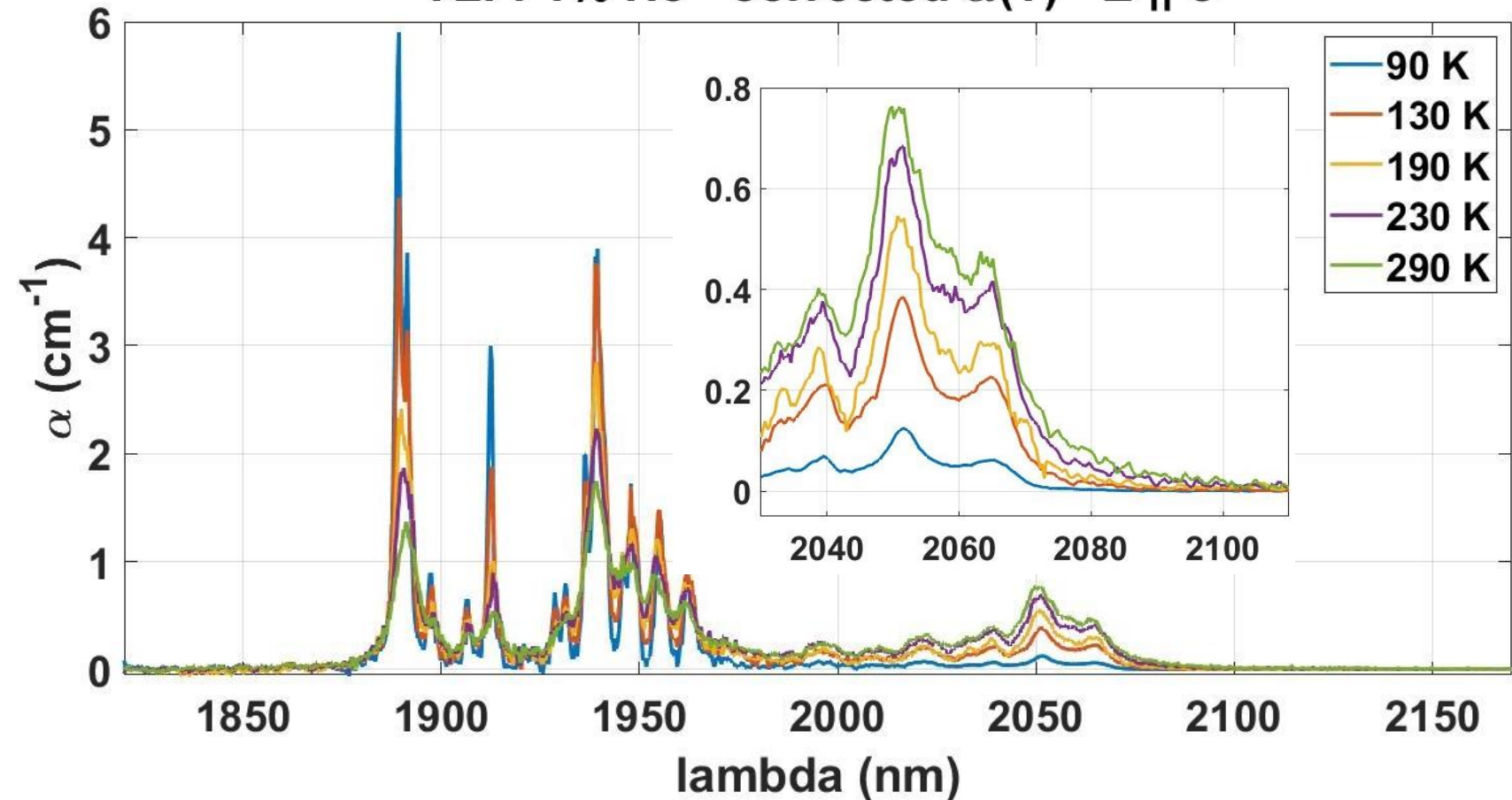


Low temperature Ho:YLF absorption results

YLF: 1% Ho - corrected $\alpha(T)$ - E || c

Parameters:

- Step: 0,3 nm
- Integration time: 3 s
- Range: 1820-2150 nm



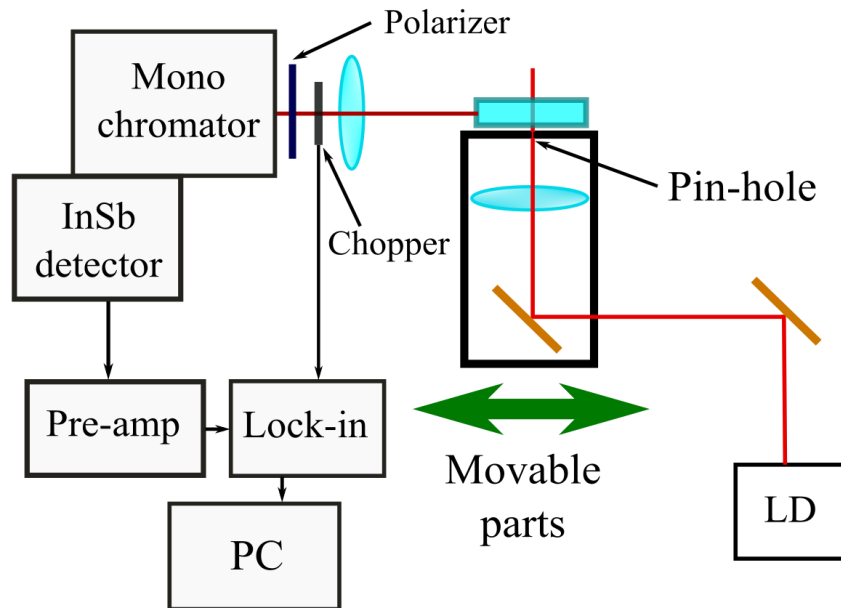
Fluorescence reabsorption setup

Sample: 0,8% Ho:YLF 9,5x5x5 mm³

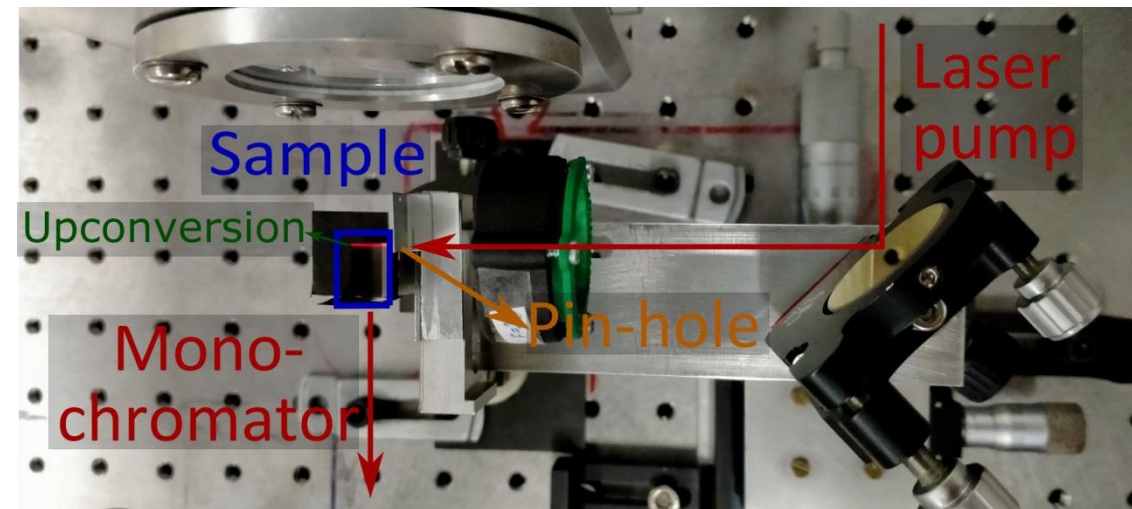
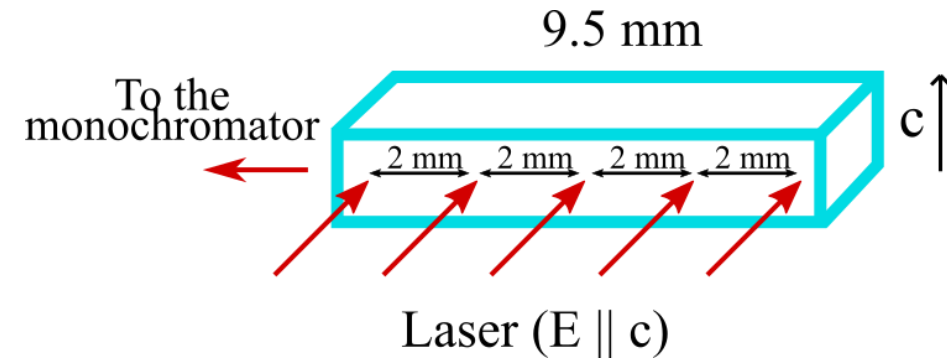
Pump: LD with $\lambda=1938$ nm, P=240 mW (after the pinhole)

Monochromator: Jobin-Yvon Triax 320

Detector: LN₂ cooled InSb detector, with a Ge LP filter (1,65 μ m)



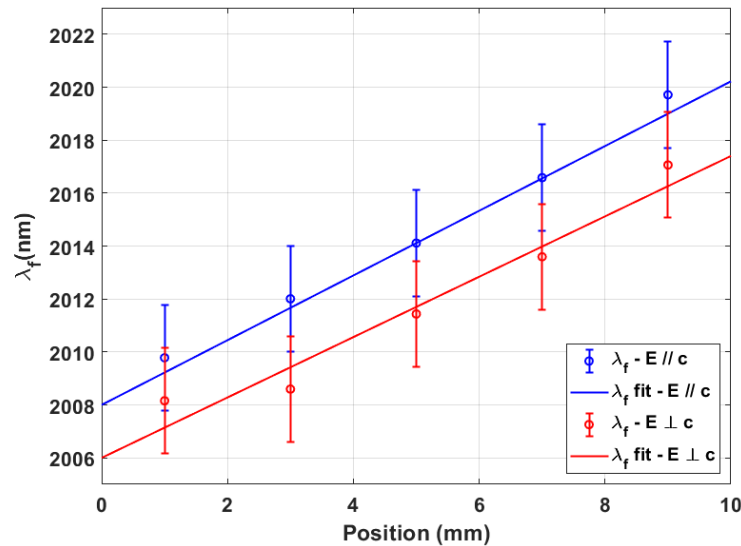
Left: sketch of the setup;
Right: detail of the movable mirror+lens+pinhole device;
Top right: detail of the sample geometry and the pump beam positions.



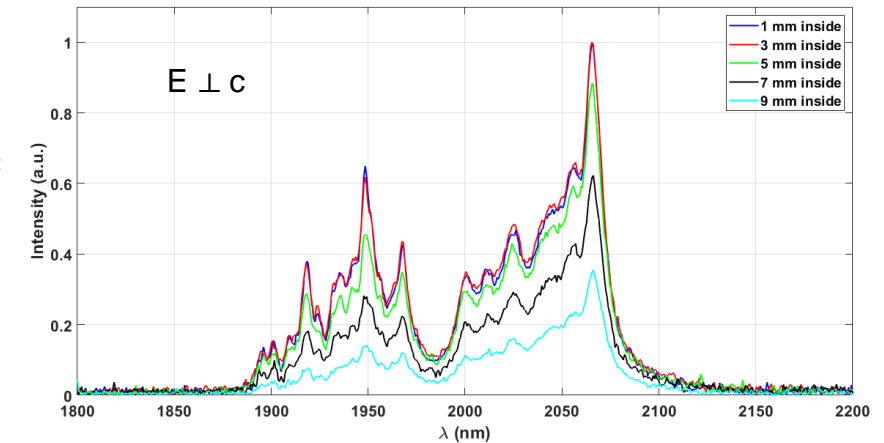
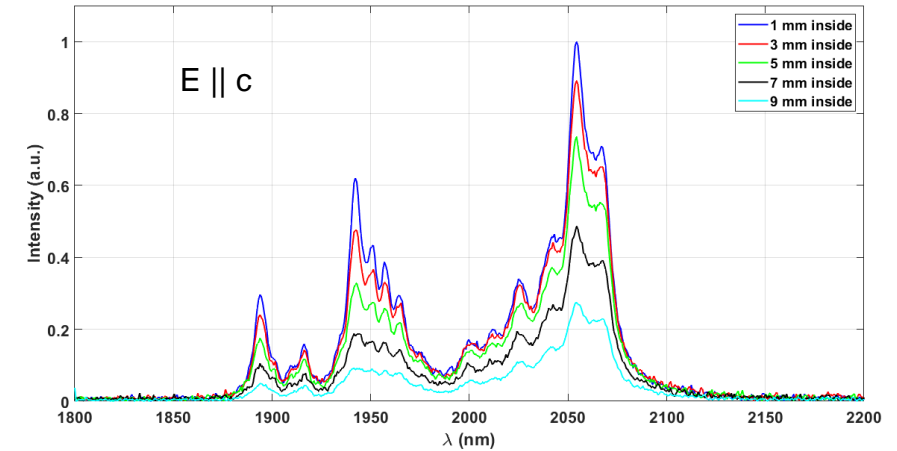
0,8% Ho:YLF Fluorescence reabsorption results

Ho $^5I_7 \rightarrow ^5I_8$ fluorescence reabsorption spectra

- monochromator slits: 0.2 mm wide;
- acquisition step: 0.7 nm;
- integration time: 1 s.



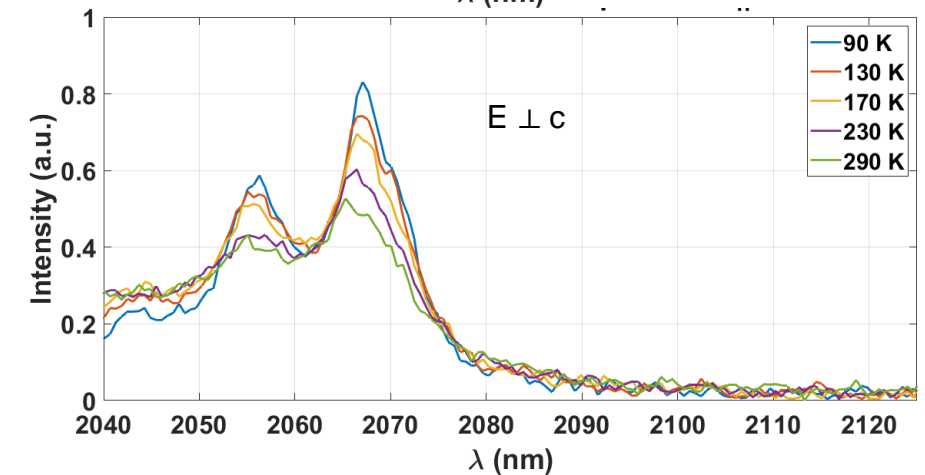
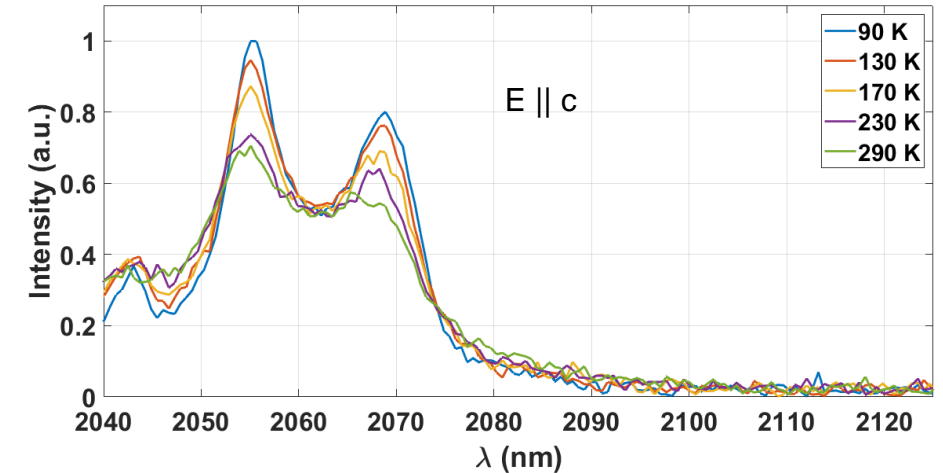
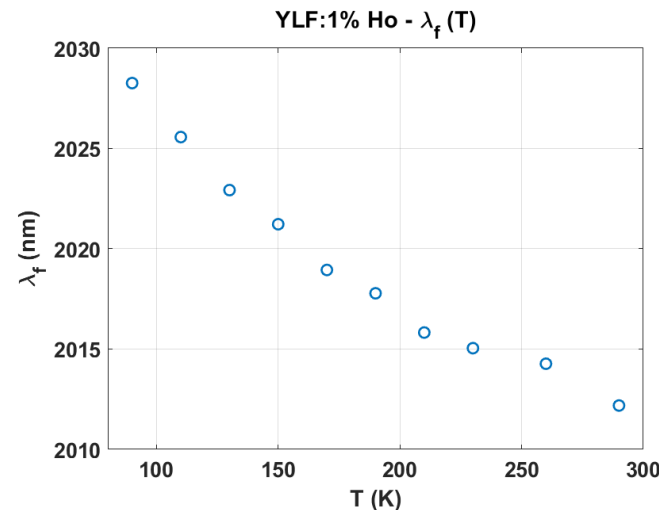
Left: Redshift of the mean fluorescence wavelength $\bar{\lambda}_f$ for 0.8% Ho:YLF as the internal reabsorption increases;
Top right: E // c fluorescence reabsorption spectra of 0,8% Ho:YLF;
Bottom right: E \perp c fluorescence reabsorption spectra of 0,8% Ho:YLF;



Low temperature 1% Ho:YLF fluorescence

- 1% Ho:YLF $^5I_7 \rightarrow ^5I_8$ transition;
- Temperature: from 290 K to 90 K
- Cryostat with CaF₂ windows;
- Monochromator slits: 0.2 mm;
- Range: 1850 - 2175 nm;
- Step: 0.600 nm;
- Integration time: 1 s;

Left: Graphical representation of the $\bar{\lambda}_f(T)$ trend for 1% Ho: YLF;
Top right: E || c low temperature fluorescence spectra;
Bottom right: E \perp c low temperature fluorescence spectra.

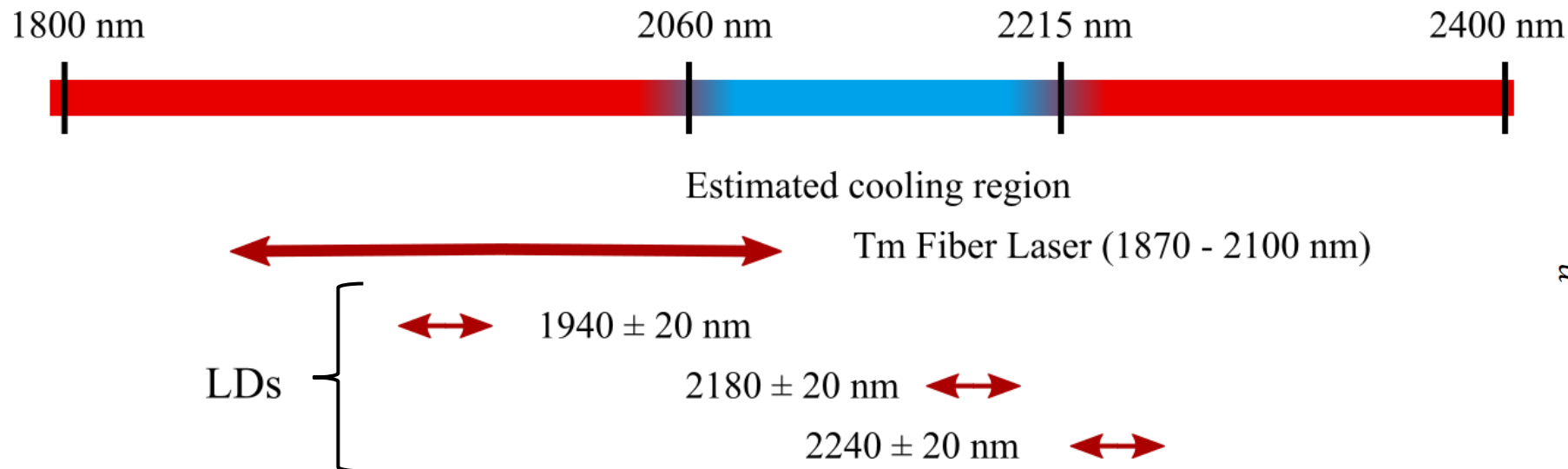


Laser sources

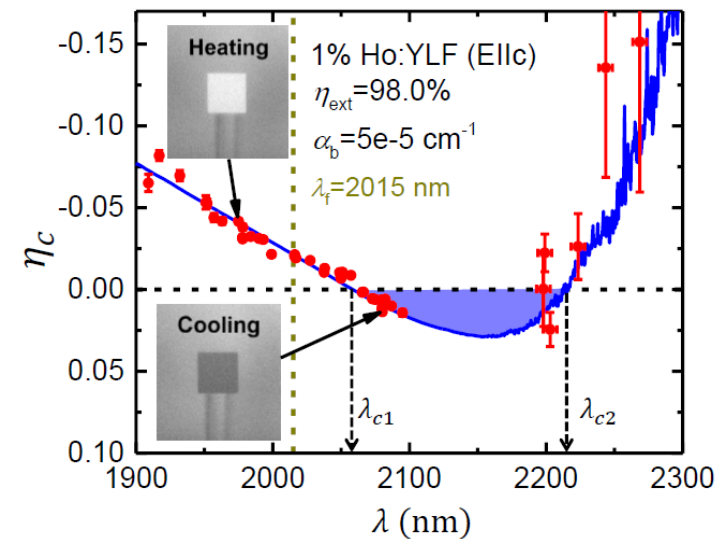
1% Ho:YLF cooling range: 2059 – 2215 nm [4]

It was decided to develop a tunable laser source around 2050 nm in collaboration with Dr. Gianluca Galzerano of Politecnico di Milano.

Additionally, laser diodes operating at other wavelengths were also purchased



Cooling efficiency and spectral range for 1% Ho:YLF [4]



Laser diodes

m2K-BA-1940-0700-SE:

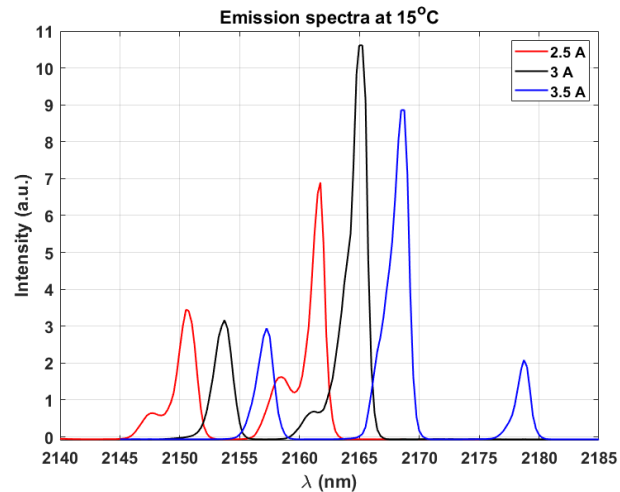
$P_{\text{max}} = 700 \text{ mW}$ at 1940 nm (LD 1940)

Coherent BA-2180-0500-CM:

$P_{\text{max}} = 500 \text{ mW}$ at 2180 nm (LD 2180)

Coherent BA-2240-0500-CM:

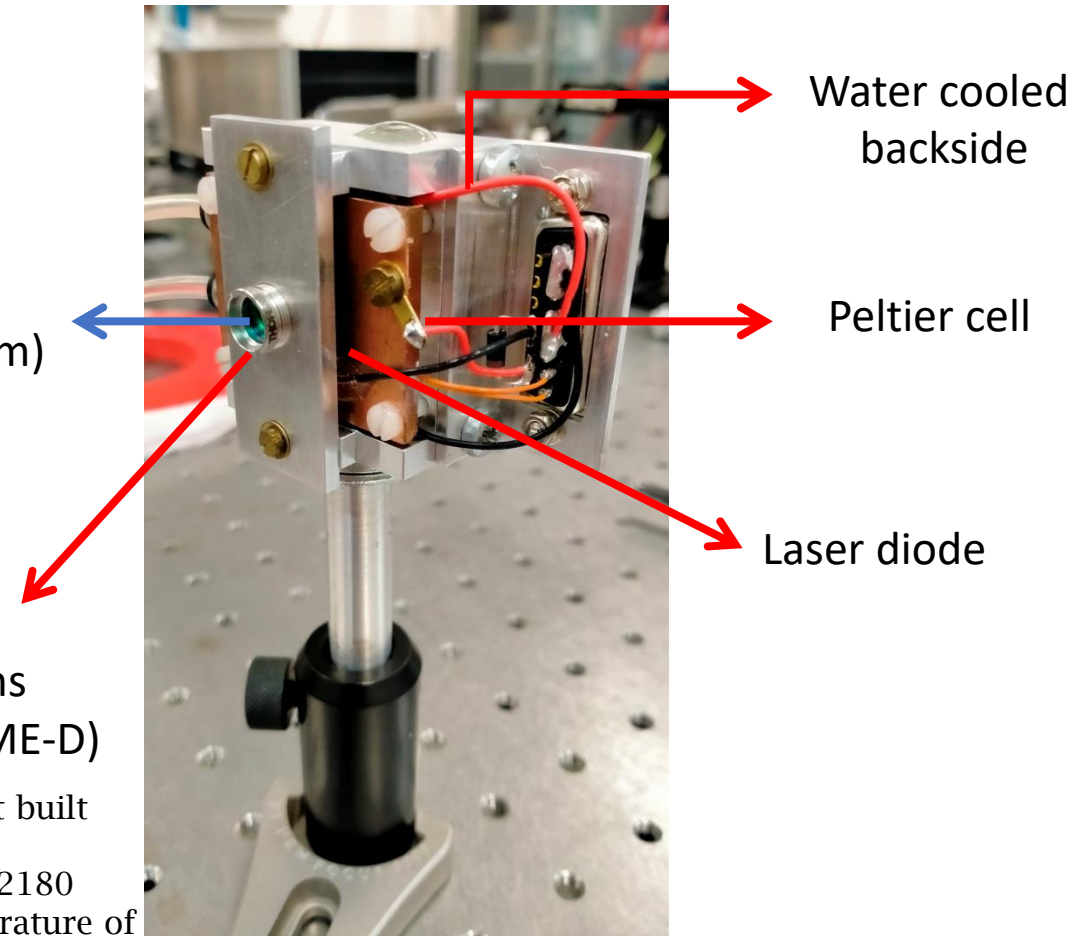
$P_{\text{max}} = 500 \text{ mW}$ at 2240 nm (LD 2240)



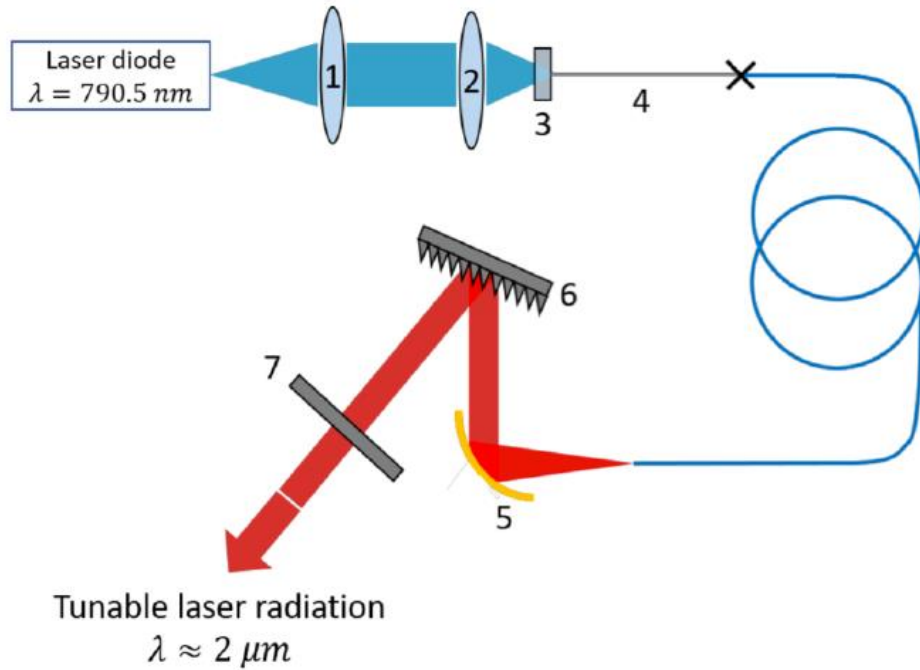
Laser output
(1940, 2180 or 2240 nm)

Collimator lens
(Thorlabs C036TME-D)

Right: custom laser diode support built for each laser diode;
Left: emission spectra for the BA-2180 laser diode at an operation temperature of 15° C



2,1 μm tunable, Tm-doped fiber laser



Emission:
1,87 – 2,1 μm , $P \approx 200 - 700 \text{ mW}$

1,5 m of
thulium-doped
fiber

1,2: Lenses

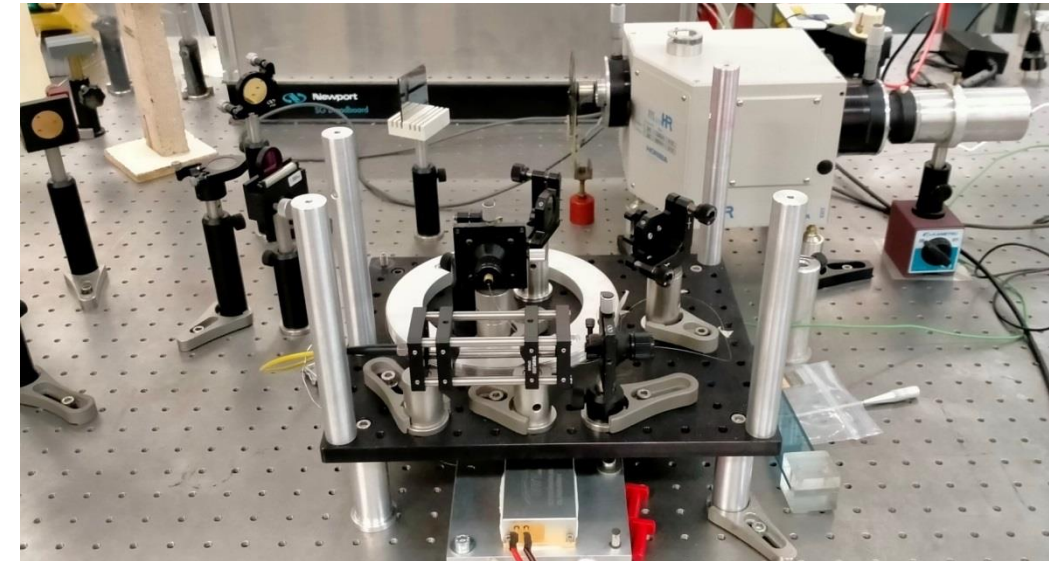
3 Dichroic mirror

4 Passive fiber

5 Golden parabolic
mirror

6 Diffraction grating

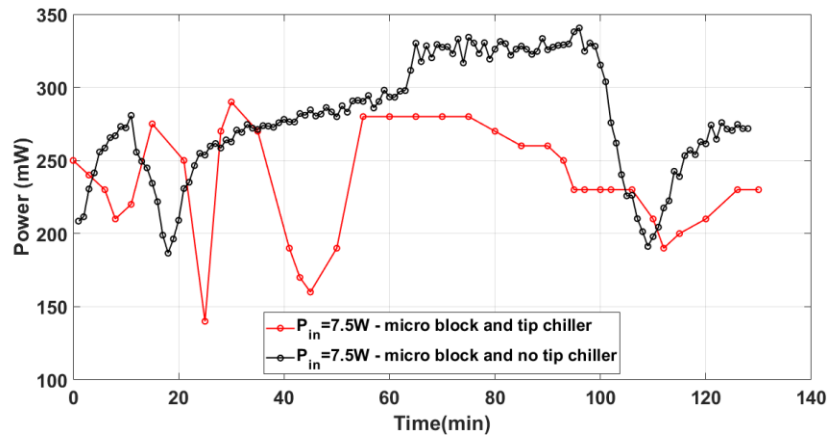
7 Output coupler



The original laser configuration

Initial configuration: high power
instabilities

Fiber laser stability – input modifications

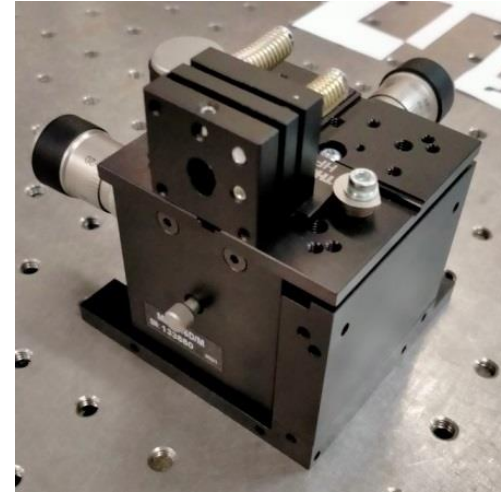


Mechanical stabilization:

1. Thorlabs MBT616D/M 3 - axis microblock compact stage (± 2 mm total travel, 300 μ m differential travel)
2. Thorlabs HFG003 adjustable flexture fiber chuck mount

Thermal stabilization:

- Homemade cooling system: aluminum cube clamped around the fiber holder connected to a solid state liquid cooler

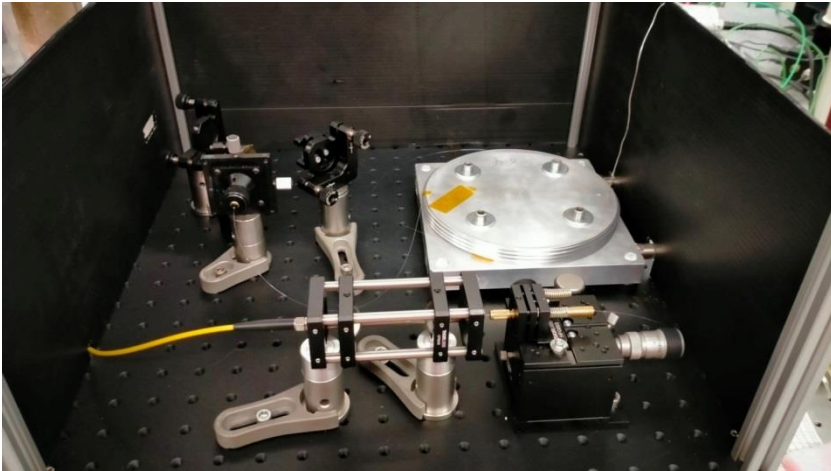


Left: power stability test with and without the tip cooling system;

Center: Thorlabs micro-block and fiber chuck mount;

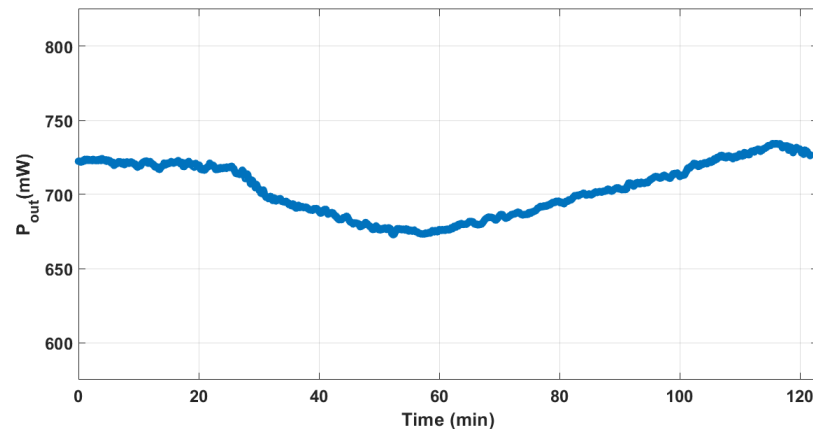
Right: the tip cooling system

Final configuration



Laser upgrade:

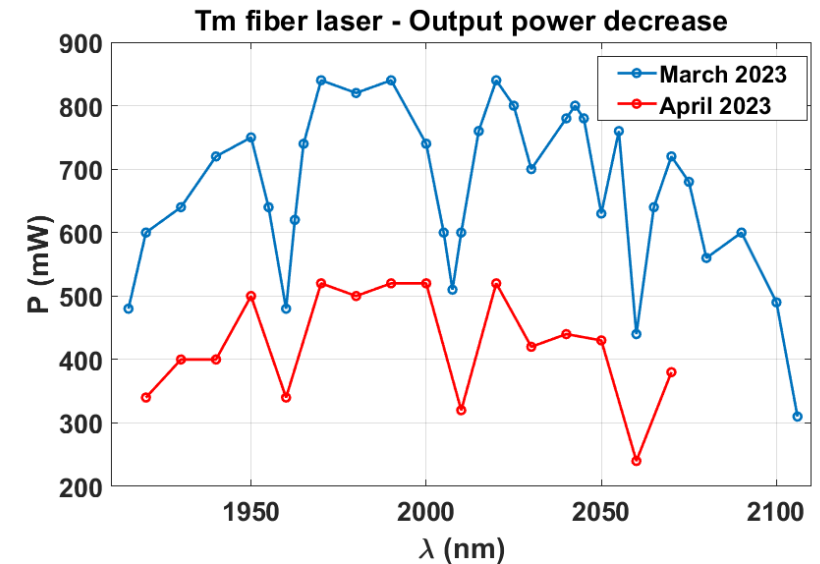
- New active medium (longer Tm^{3+} -doped fiber) to increase power at longer wavelengths;
- New active medium cooling system (cooling plate and a fiber holder) to increase power stability.



Top left: picture of the laser in its final configuration;

Bottom left: stability of the Tm-doped fiber laser after the cooling system for the active fiber was implemented ($\lambda = 2070$ nm);

Right: output power of the Tm-doped fiber laser with the new, longer active fiber. The blue graph represents its best output, while the red one represents the output after its power decreased.



Optical refrigeration at 2 μm

- LITMoS setup
- Thermal camera calibration
- Experiments on Ho:YLF
- Experiments on Tm:YLF

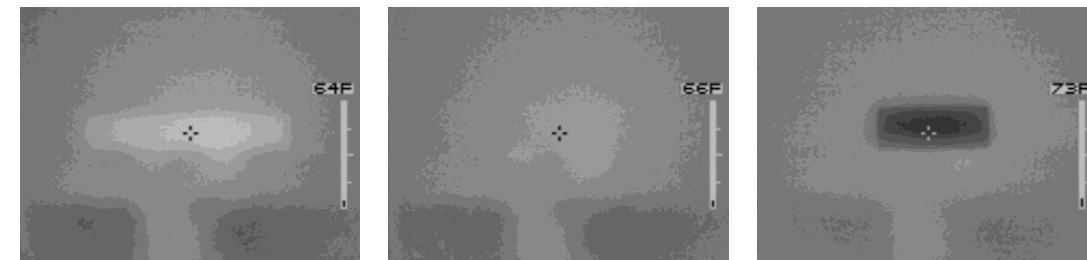
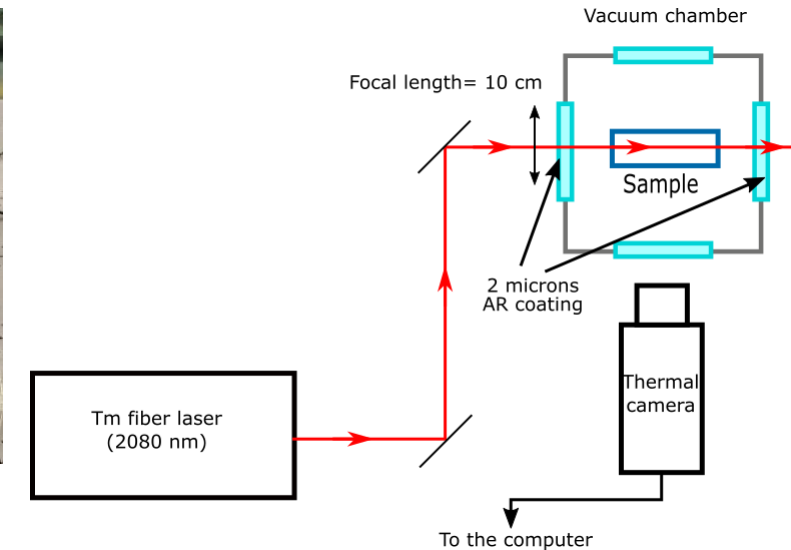
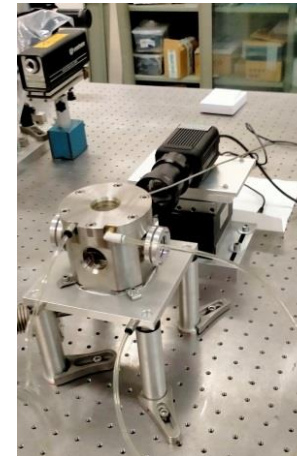
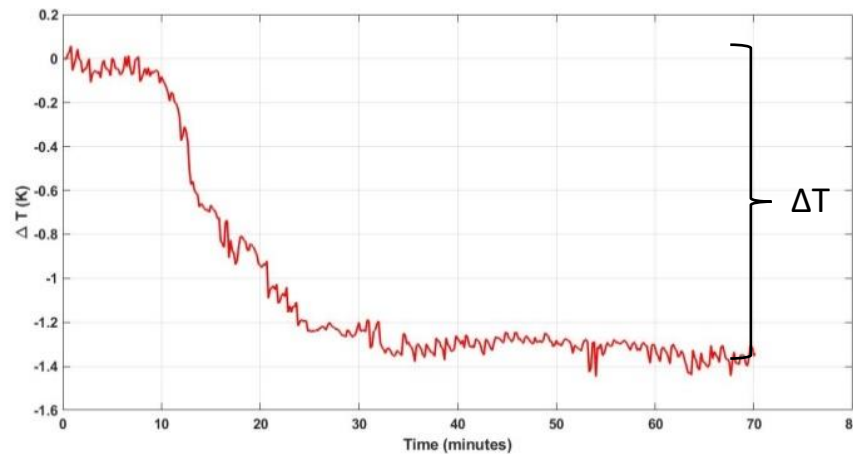
Optical refrigeration LITMoS setup

LITMoS: Laser-Induced Thermal Modulation Spectroscopy

- Vacuum chamber with a thermally insulated sample holder (minimize conduction and convection)
- Monitor sample temperature with a thermal camera (COX CG320) as it is pumped with a laser beam

Top Right: scheme of the experimental setup, with a picture of the thermal camera and the vacuum cell;

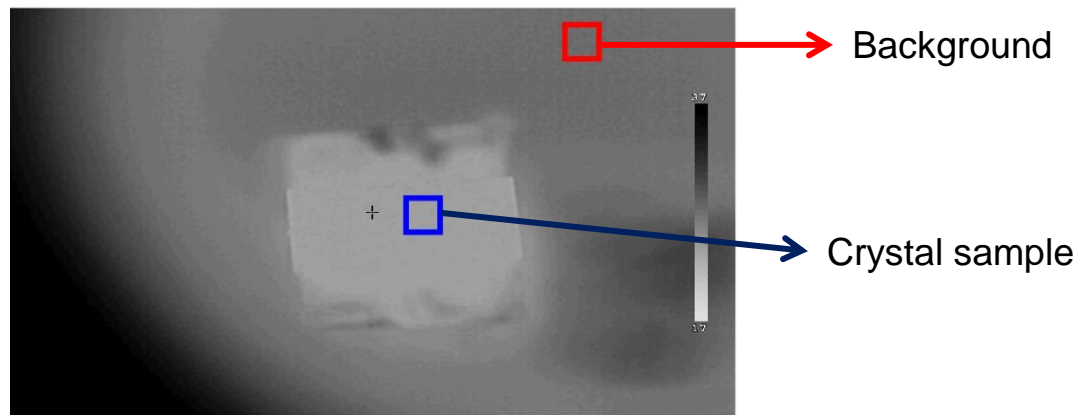
Bottom Right: an example of a LITMoS experiment. From left to right, a temperature graph extrapolated from the thermal camera video, a video frame of a cooling crystal (white), a frame of a crystal at room temperature (grey), and a frame of a heating crystal (black)



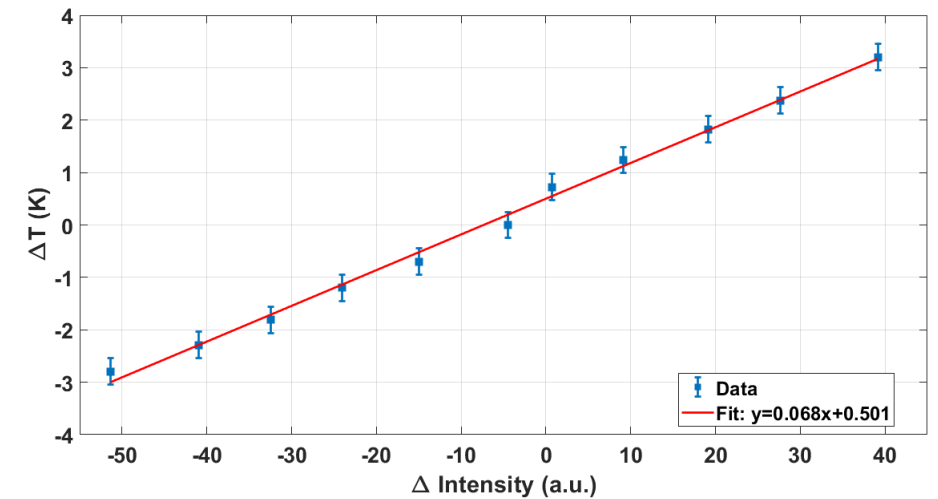
Thermal camera calibration

To accurately measure the temperature of the YLF crystal samples, the pixel intensity of a small YLF crystal was registered at different, known temperatures, along with the chamber background temperature. The crystal was attached to a Peltier cell (to control its temperature), and a series of thermocouples allowed us to register all the required temperatures. The following calibration function was obtained:

$$\overline{\Delta T}(K) = \overline{\Delta I} \cdot (0,06814 \pm 0,0034) + (0,5011 \pm 0,0969)$$



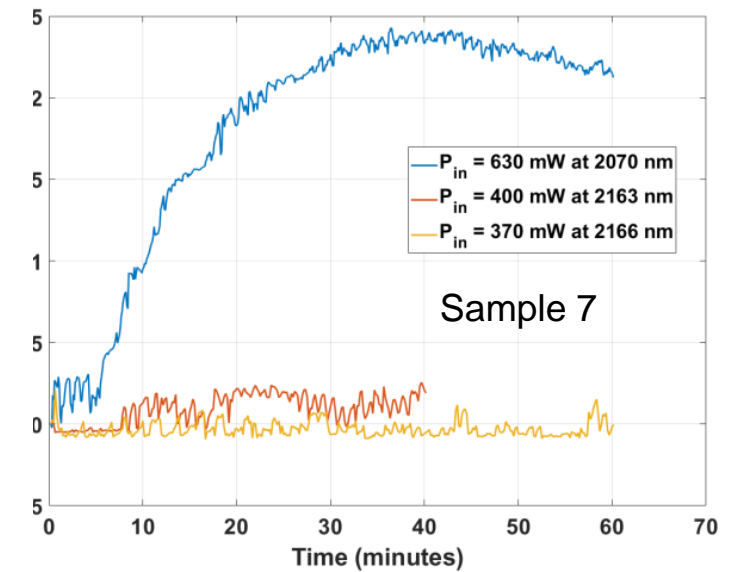
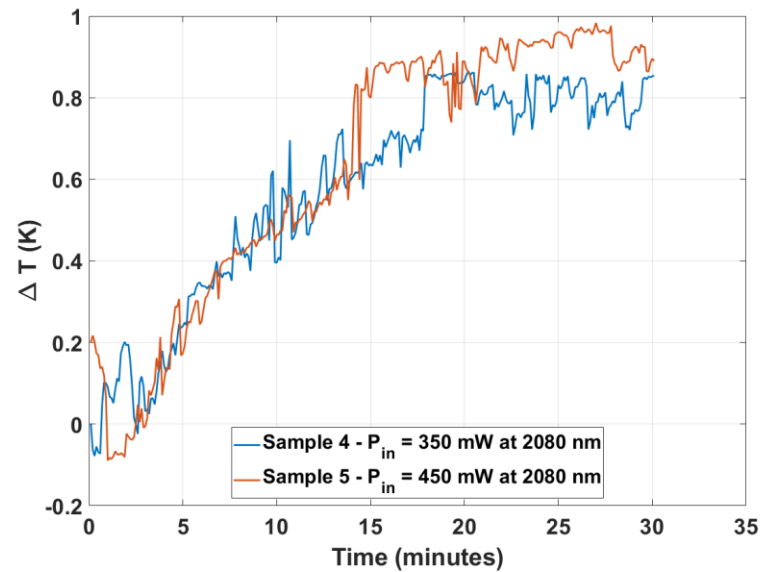
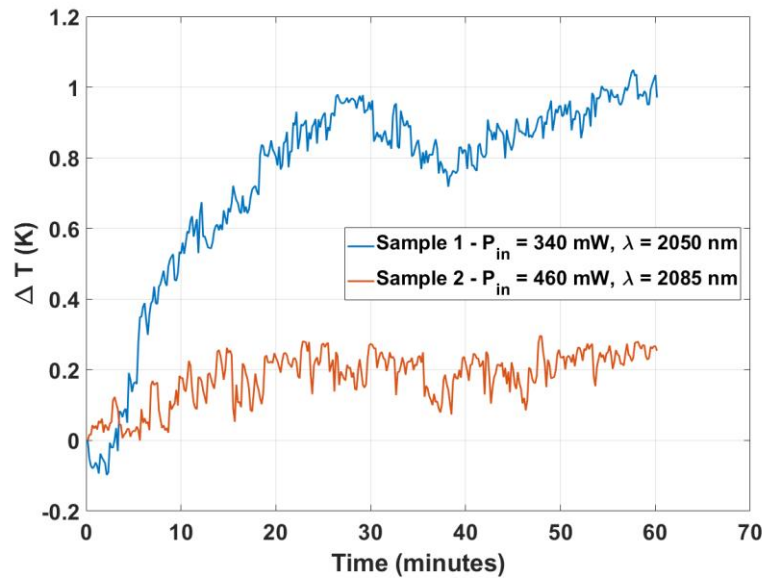
An example of a frame registered during the calibration measurements



Plot of the recorded data and the calibration fit we obtained

Ho:YLF LITMoS results

- **0,8% Ho :YLF**
 - Sample 1
 - Sample 2
 - Sample 3
- **1% Ho:YLF**
 - Sample 4
 - Sample 5
 - Sample 6
 - Sample 7 (cut from sample 6)

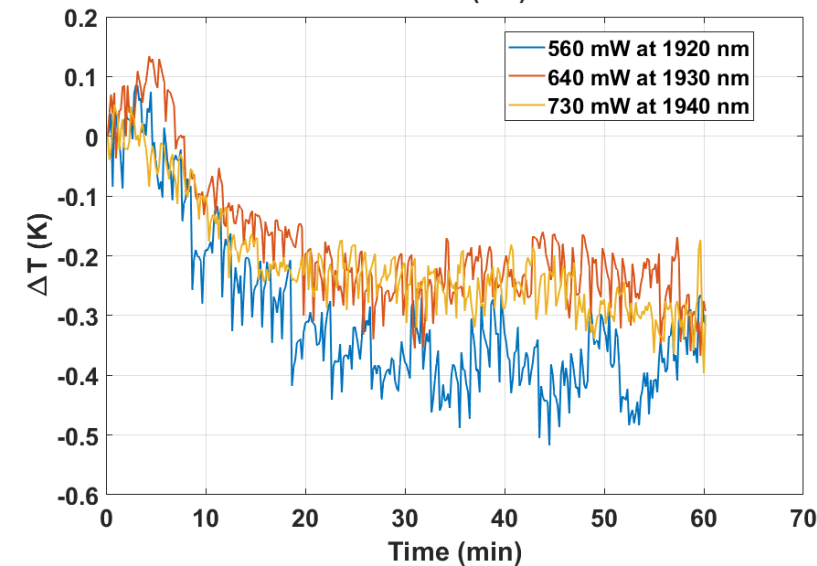
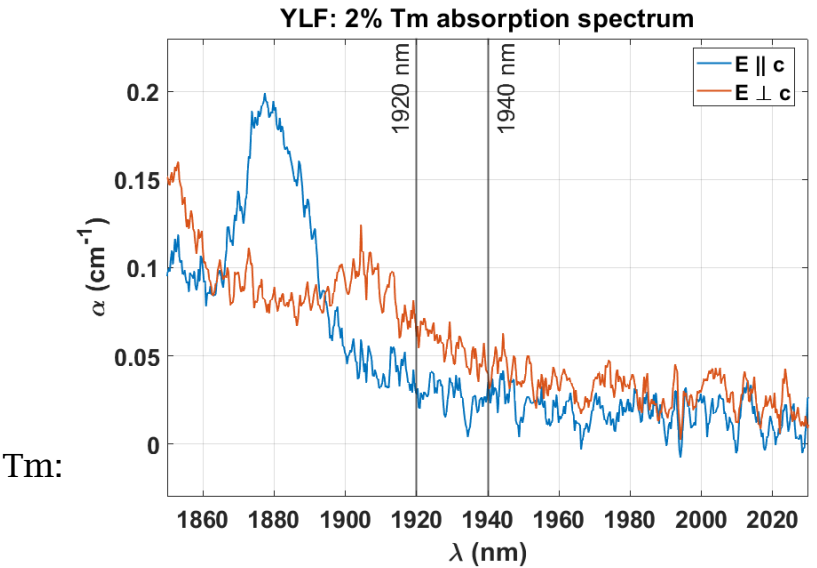
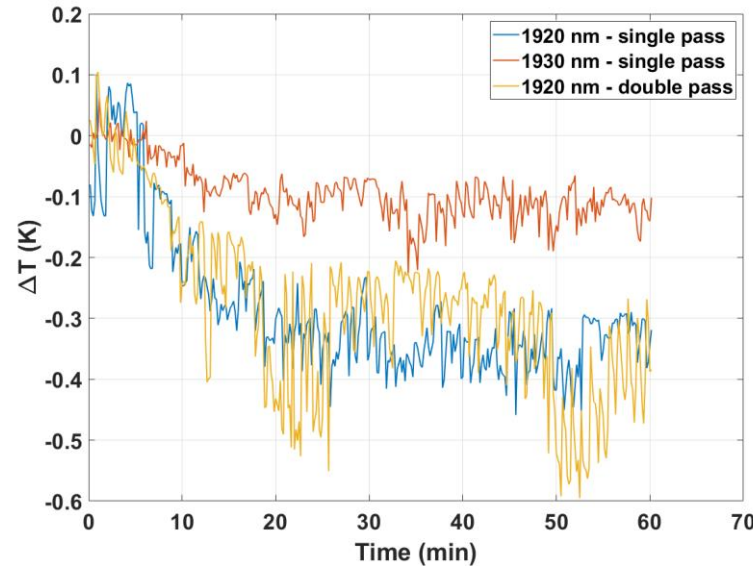
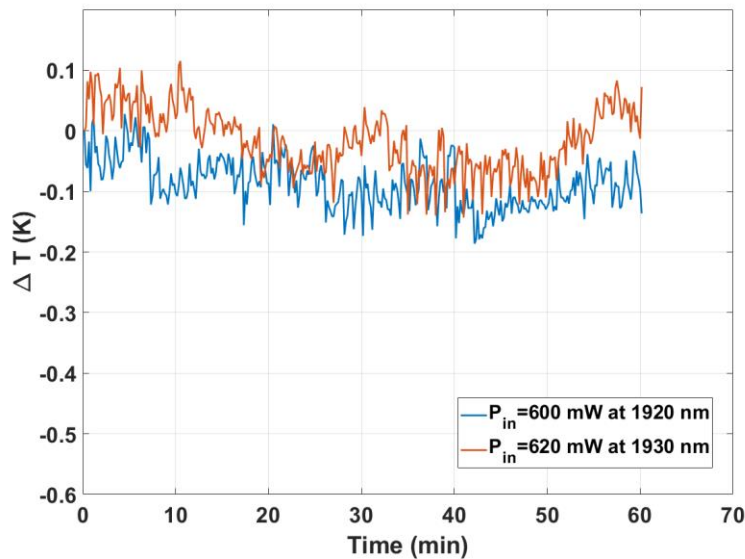


Tm:YLF refrigeration results

Since our tunable fiber laser had good power (up to 1 W) at 1920-1940 nm, we tried to cool down some Tm:YLF samples. These are the results.

Left: 2% Tm:YLF absorption spectrum (top)

Bottom (from left to right): cooling of 1% Tm:YLF ($E \parallel c$, left, and $E \perp c$, center), and cooling of 2% Tm:YLF ($E \perp c$, right)



Optical refrigeration at 1 μm

- The parallel configuration
- Cryostat for temperature – controlled LITMoS

Parallel configuration

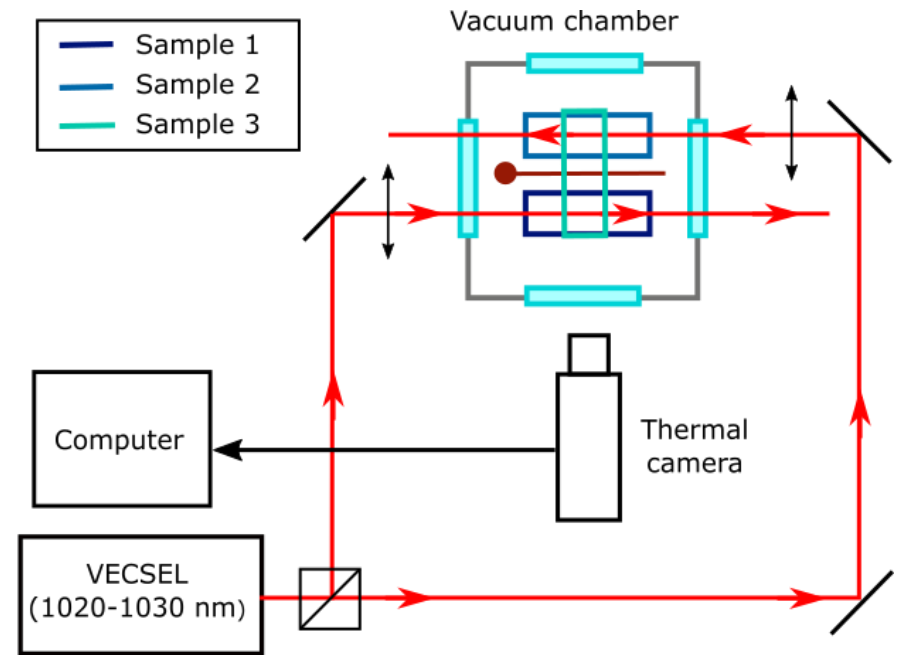
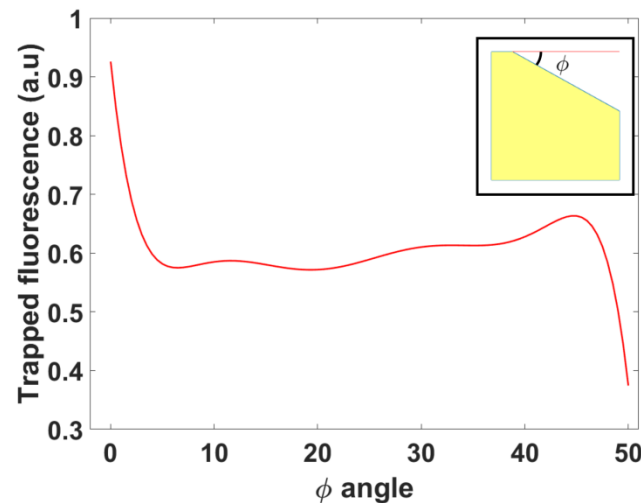
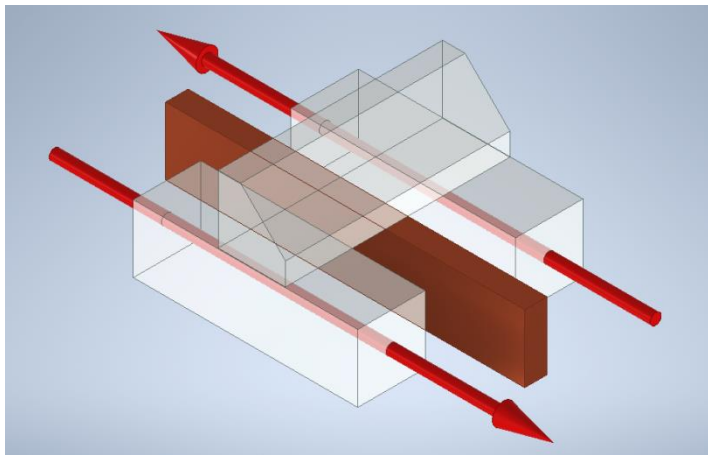
Advantage: Increase cooling power while avoiding saturation.

Sample 1: 5% Yb:YLF (active sample)

Sample 2: 5% Yb:YLF (active sample)








Sample 3: undoped YLF (thermal link)

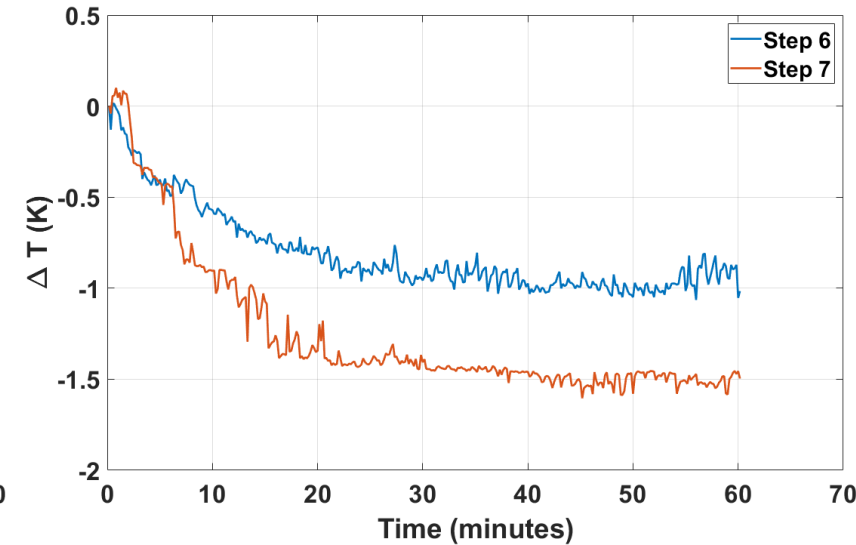
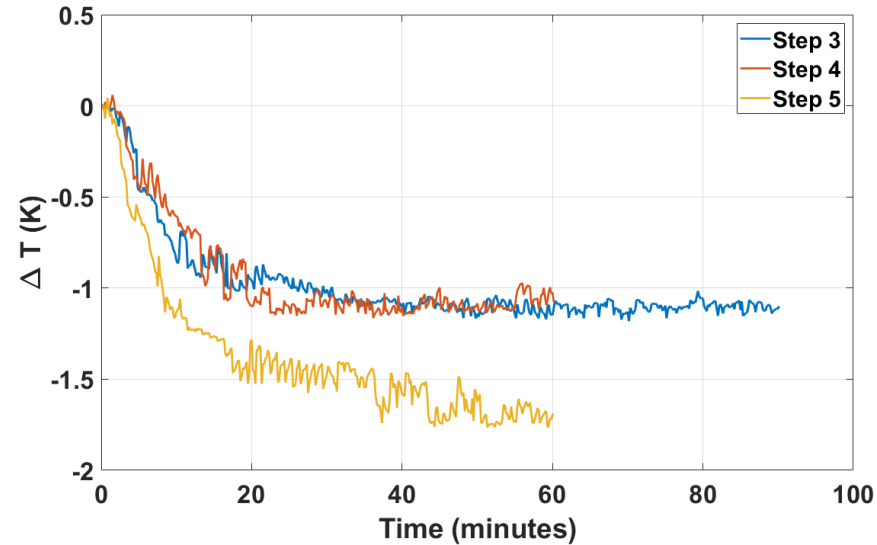
The shape of sample 3 was modified to reduce fluorescence trapping (see below).



Top: scheme of the parallel configuration setup;
Center: simulation of the amount of trapped fluorescence within the thermal link as a function of the slope angle of the top facet;
Left: 3D model of the 2 active samples with the thermal link on top and a copper screen between them (the red arrows represent the two laser beams pumping the samples).

Parallel configuration - results

Step	Configuration	Samples used	Cooling power	Theoretical expectation	Experimental $\Delta T(K)$
1		1	P_{cool}	ΔT	-2.0 ± 0.1
2		2	P_{cool}	ΔT	-1.9 ± 0.1
3		1 and 3a	P_{cool}	$\frac{\Delta T}{2}$	-0.9 ± 0.1
4		1 and 3b	P_{cool}	$\frac{\Delta T}{2}$	-1.1 ± 0.1
5		1 and 3b	$2 P_{cool}$	ΔT	-1.7 ± 0.1
6		1, 2 and 3a	$P_{cool} + P_{cool}$	$\frac{2\Delta T}{3}$	-1.0 ± 0.1
7		1, 2 and 3b	$P_{cool} + P_{cool}$	$\frac{2\Delta T}{3}$	-1.5 ± 0.1



Left: table with the list of configurations that were tested, the amount of cooling power that was generated each time, the expected temperature drop, and the experimental result that was measured;

Top (center and right): temperature shift plots for configurations 3 to 7; the right figure shows how the change from sample 3a to sample 3b improved the actual cooling performance of the setup.

Cryostat for temperature-controlled LITMoS

Both absorption and emission spectra depend on the temperature of the sample. So, it would be interesting to be able to test crystal samples for cooling not only at room temperature.

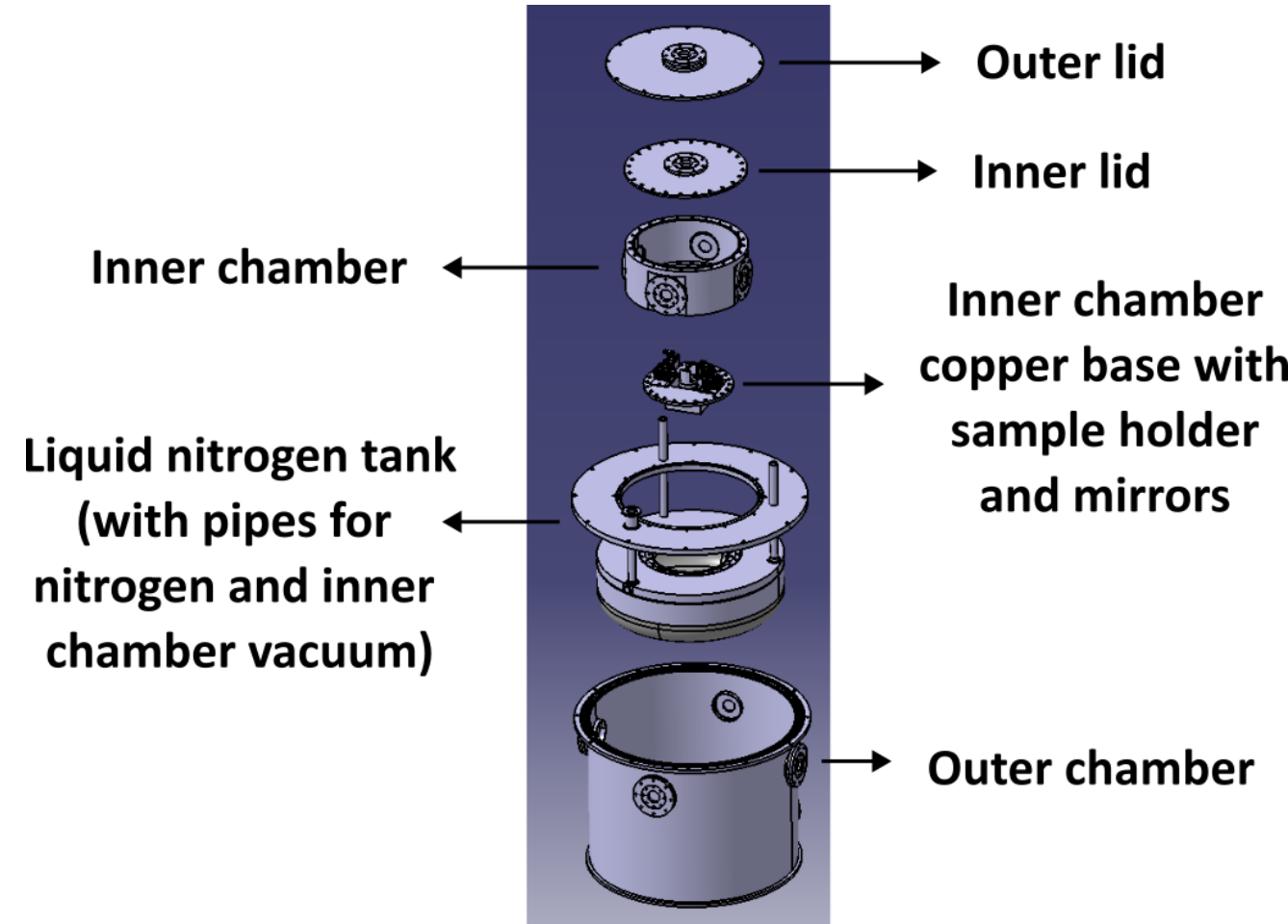
Requirements	Solution
LITMoS experiment	Sample is thermally insulated when excited by the laser
Fluorescence experiments	Multiple windows to monitor the sample
Experiments at different temperatures (from 290 K to 77 K)	<ul style="list-style-type: none">• LN tank connected to the chamber• He as an exchange gas• Temperature controller in the sample holder
Multi-pass configuration to increase laser absorption	<ul style="list-style-type: none">• Mirrors near the sample• Telescope to adjust the laser beam
Usable in different optical ranges	Interchangeable optics and windows
Movable	

Cryostat structure

During the design of the cryostat, several designs were considered to meet our requirements and at the same time to ensure:

- thermal insulation
- physical integrity (vacuum/pressure)
- low temperature vacuum seals

This led to what has become its final structure.



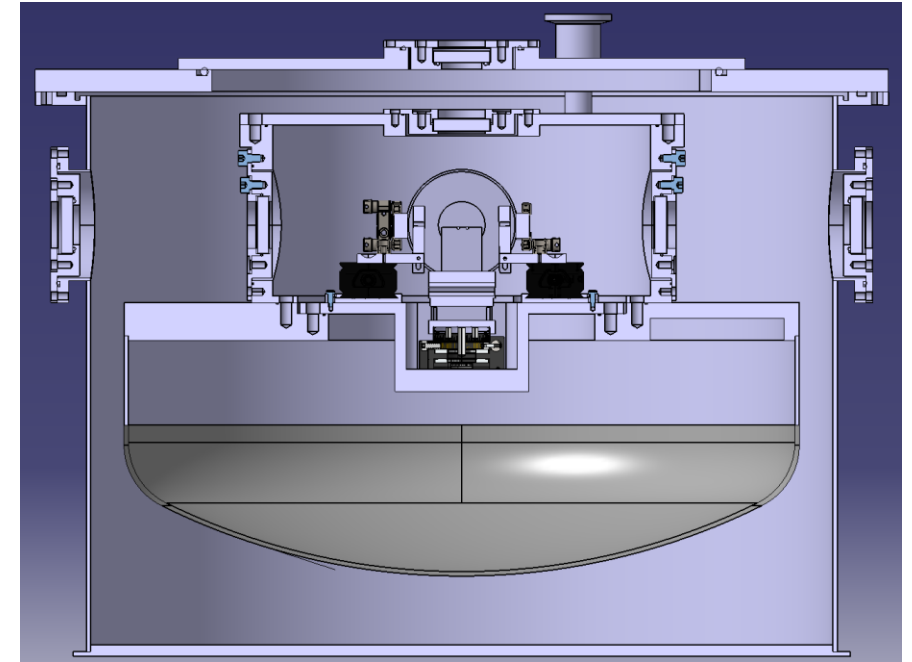
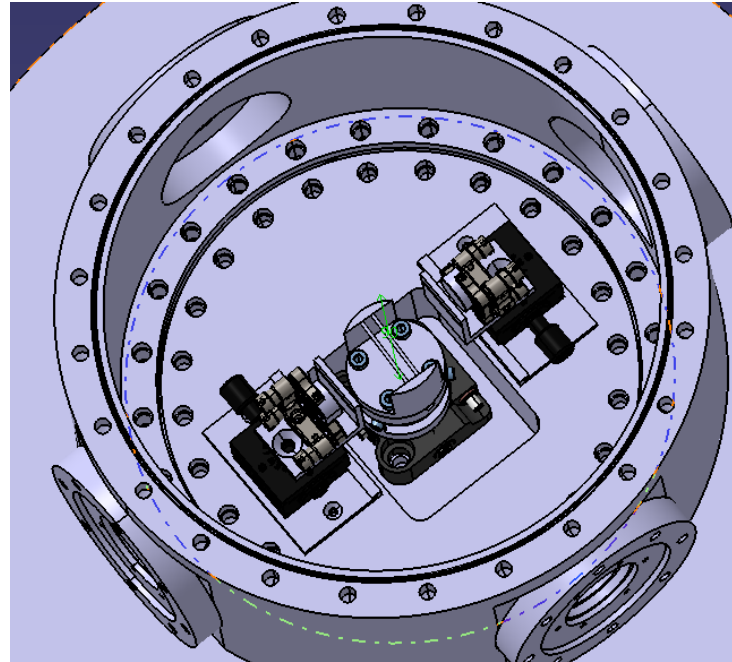
Final design

Cryostat size :

- External diameter ≈ 400 mm
- Height ≈ 270 mm
- Inner chamber diameter ≈ 200 mm
- LN tank ≈ 6 L

Center: view from above of the inner chamber with the sample holder and the mirrors on their translators;

Right: section view of the cryostat along the plane where the laser beam should pass.



Laser beam simulations

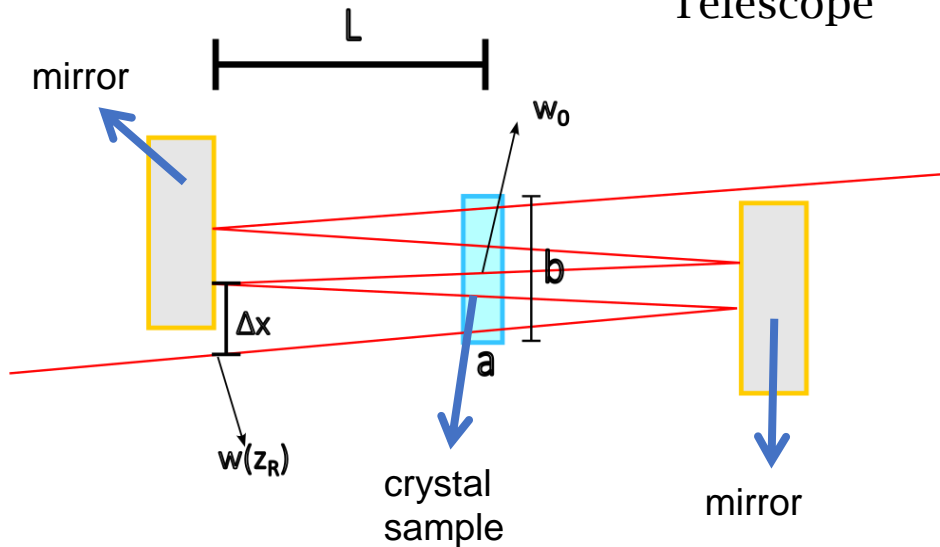
Size of the cryostat



Constraints on the laser beam parameters (waist size and position, beam divergence...)



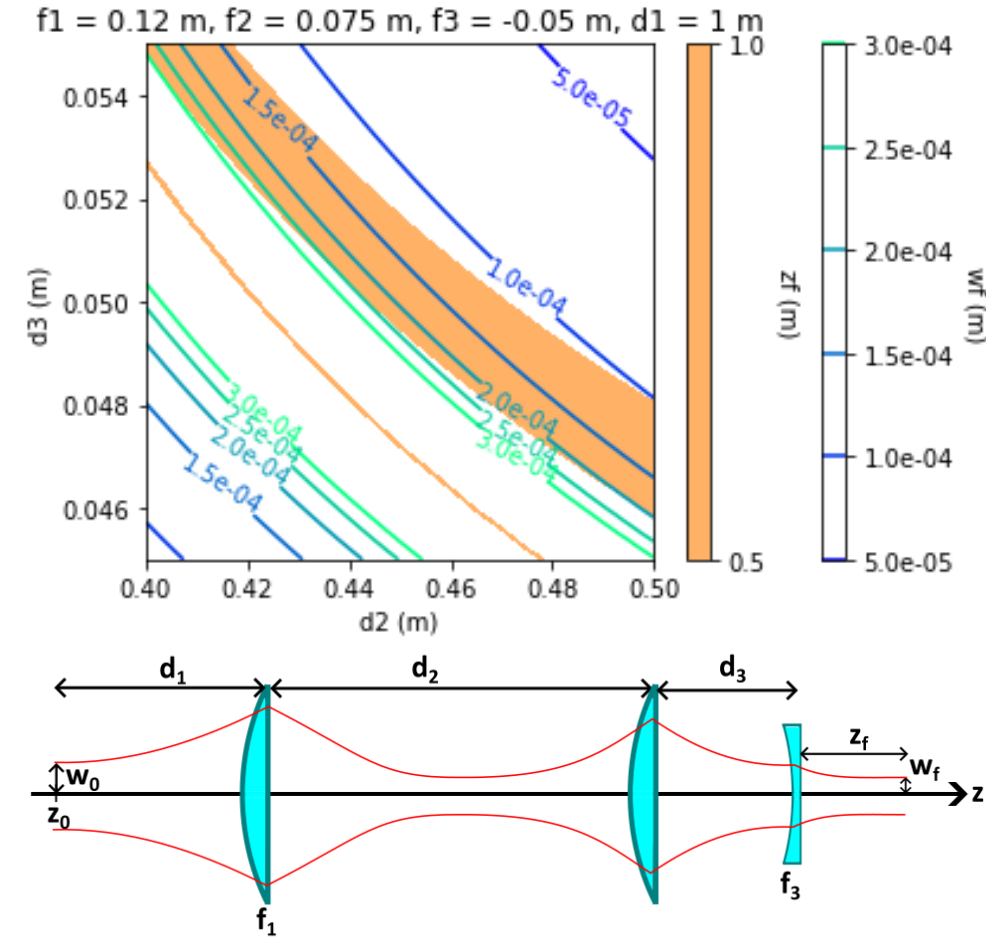
Telescope



Left: scheme of the multipass setup (seen from above), with the sample between two plane mirrors;

Top right: results of the beam propagation simulations; the orange area is where the output beam from the telescope has a waist between 0,5m and 1 m from the final lens;

Bottom right: scheme of the telescope with its parameters.



Conclusions

- Growth of 3 boules: 1 boule of 0,8% Ho:YLF, 2 boules of 1% Ho:YLF
- Optical characterization:
 - Absorption spectra: $\alpha < 0,2 \text{ cm}^{-1}$ for $\lambda > 2070 \text{ nm}$;
 - Mean fluorescence wavelength: $\bar{\lambda}_f = 2009 \text{ nm}$ for 0,8% Ho:YLF, $\bar{\lambda}_f = 2012 \text{ nm}$ for 1% Ho:YLF;
 - Fluorescence reabsorption: $\bar{\lambda}_f$ increases up to 2020 nm for 0,8% Ho:YLF if the laser beam is at 9 mm from the surface;
 - Low temperature experiments: absorption and emission change as temperature decreases;
 - Mean lifetime of Ho $^5\text{I}_7$ manifold: 15,4 ms;
- Tm-doped fiber laser prototype: reached 500 mW at 2090 nm, but presented stability and reliability issues;
- Tested 7 samples of Ho:YLF (between 0,8% and 1%): none of the samples cooled down;
- Tested Tm:YLF samples for optical refrigeration around 1930 nm: $\Delta T = -0,2/0,3 \text{ K}$;

Conclusions (2)

- Investigated the potential of a parallel cooling configuration with Yb:YLF samples to increase overall cooling power while avoiding saturation;
- Design of a cryostat for temperature – controlled LITMoS experiments; design was completed and cryostat is being fabricated and tested

Furhter developments:

- An adequate laser source is necessary to systematically investigate the cooling potential of Ho:YLF; the source should reach 2100-2150 nm with about 1 W of power. Potential candidates could be Ho:Tm solid state lasers, or OPOs using non-linear crystals;
- Test samples at different pump intensities to explore the impact of cooperative mechanisms on the cooling efficiency.

Publications

- Francesco Caminati, Giovanni Cittadino, Eugenio Damiano, Alberto Di Lieto, and Mauro Tonelli, "**Loss processes on crystal cooling efficiency**", Opt. Express 29, 41313-41322 (2021);
- Francesco Caminati, Giovanni Cittadino, Eugenio Damiano, Alberto Di Lieto, and Mauro Tonelli, "**A design for optical refrigeration: the parallel configuration**", Applied Physics Letters, Vol. 122, Iss. 2 (2023).

Acknowledgments – Pisa

University of Pisa crystal growth lab /
MEGA Materials S.r.l.:

- Prof. Mauro Tonelli
- Prof. Alberto Di Lieto
- Dr. Giovanni Cittadino
- Dr. Eugenio Damiano
- Davide Baiocco
- Fabio Torri
- Ilaria Grassini
- Alessandro Masetti



Acknowledgments - Grenoble

Institut Néel – CNRS

- Dr. Gilles Nogues
- Enzo Joud
- Laurent Del Rey
- Julien Jarreau
- Didier Dufeu
- Jérôme Debray



Air Liquide Advanced Technologies:

- Dr. Arnaud Gardelein



In memory of Dr. Bauke Heeg



Itens – 16th July 1969

Leeuwarden – 4th April 2025

Thank you very much for your attention



**UNIVERSITÀ
DI SIENA**
1240

References

1. D. V. Seletskiy, et al., "Cryogenic optical refrigeration", Advances in optics and photonics, 4:78–107, 2012.
2. D. V. Seletskiy, et al., "Laser cooling of solids to cryogenic temperatures", Nat. Photonics, 4(3):161–164, 2010.
3. G.-Z. Dong and X.-L. Zhang, "Role of upconversion in optical refrigeration: A theoretical study of laser cooling with Ho^{3+} doped fluoride crystals", J. Opt. Soc. Am. B, 30(11):3041–3047, 2013.
4. S. Rostami, A. R. Albrecht, A. Volpi, and M. Sheik-Bahae, "Observation of optical refrigeration in a holmium-doped crystal", Photon. Res., 7(4):445–451, Apr 2019;